EVALUATION OF FEATURES AND QUANTITATIVE ASSESSMENT OF HEMIPARETIC UPPER-LIMB MOVEMENT THROUGH PHASE PLANE ANALYSIS

by

MINOOSH K. MORADI

A dissertation submitted to the

Graduate School-New Brunswick

Rutgers, The State University of New Jersey

and

The Graduate School of Biomedical Sciences

In partial fulfillment of the requirements

For the degree of

Doctor of Philosophy

Graduate Program in Biomedical Engineering

Written under the direction of

William Craelius, Ph.D.

And approved by

_____

_____

_____

_____

New Brunswick, New Jersey

OCTOBER 2015

ABSTRACT OF THE DISSERTATION

Evaluation of Features and Quantitative Assessment of Hemiparetic

Upper-Limb Movement through Phase Plane Analysis

By MINOOSH K. MORADI

Dissertation Director:

William Craelius, Ph.D.

Neurological disorders or cerebrovascular accidents can affect one's ability to perform activities of daily living, requiring a team of specialists to assess the condition and plan proper treatment. However, current methods used to evaluate aspects of motor impairment are subjective, which may lead to inconsistent and inaccurate assessments and ultimately affect the therapy protocol. Herein, focus was directed toward the development of an objective, reliable metric based on quantification of motion presented in the phase domain.

To begin, representations of single-joint extension-flexion were examined to assess graphing features that become more prominent with impaired motion. From this work, it was shown that alternative methods of displaying movement data retain features that distinguish impaired movement, while providing a distinct visual record for quick comparison. Further work focused on the development of a novel scheme—based on computational geometry—for quantifying the area enclosed by complex phase portraits, validation of its performance (*accuracy, sensitivity, specificity > 96%*), and application in a metric of motor performance, the Phase Area Ratio (PAR). The final focus

demonstrated the use of PAR to track progression of SPMS subjects, receiving anti-spasticity drug treatment. PAR did not improve significantly in the upper extremities between the baseline test session and the one-month follow up test session, but it was revealed that scores were significantly dependent on the movement pace.

It is concluded that phase portraits provide a viable means to capture and quantify the idiosyncrasies of human movement and are a useful tool for tracking progression of hemiparetic individuals through treatment.

ACKNOWLEDGEMENT

I would like to thank my advisor, Dr. William Craelius, for giving me the opportunity to work under his direction. He gave me the freedom to explore my own path, guidance to overcome barriers that fell at my feet, and motivation as I made it down the final stretch.

Also, I would like to thank my committee members, each contributing uniquely to my experience. First, I am greatly appreciative of Dr. Troy Shinbrot for awakening my senses and reminding me that common items are often wondrous, if time is taken to truly observe. Also, a special thanks goes to Dr. Kang Li for his willingness to be direct and share his perspective; his intentions were to always keep me on the most efficient and effective path. Finally, I am thankful for Dr. Mitch Wallin, who not only made the VADC study possible but also readily provided his clinical expertise.

Throughout my time in the Biomechanics and Rehabilitation Engineering Lab, many, many labmates have come and gone—each one fantastic and unforgettable. I credit their passion as the reason that I was drawn toward both the lab and to Rutgers. Each has offered continual, genuine friendship, even years after their departure, and I cannot imagine this experience without any one of them.

On a final note, this dissertation would not have been possible without my family and really no words can express my gratitude toward them. Since a very young age, I have been encouraged to learn anything and everything, reminded of my strengths and loved beyond limits. My parents and siblings have been the greatest supporters and role models, and without them, I would not have realized my potential.

DEDICATION

I dedicate this dissertation to my favorite three—AJ, TP, and WJ. They have spent every day of their lives alongside me in this journey. Their spontaneity kept me in the moment, never the time to dwell on the past or get lost in the future. Although each day offered a unique challenge, it also offered more laughter and happiness than I have ever known.

TABLE OF CONTENTS

ABSTRACT ii
ACKNOWLEDGEMENT iv
DEDICATION v
LIST OF TABLES viii
LIST OF FIGURES ix
CHAPTER 1: GENERAL INTRODUCTION 1
UPPER MOTOR NEURON SYNDROME AND SPASTICITY 1
TREATMENT 3
ASSESSMENT 4
STATEMENT OF NEED 6
HYPOTHESES 6
HYPOTHESIS 1: 7
HYPOTHESIS 2: 7
HYPOTHESIS 3: 7
THESIS OVERVIEW 7
CHAPTER 2: HUMAN MOTION ANALYSIS USING SPATIO-TEMPORAL REPRESENTATION 9
ABSTRACT 9
INTRODUCTION 10
METHODS 13
SUBJECT POOL 13
INSTRUMENTATION AND TEST PROTOCOL 13
SIGNAL PROCESSING 14
TEMPORAL & PHASE PLOT FEATURE ASSESSMENT 14
FEATURE DEFINITIONS 16
FEATURE ASSESSMENT AND STATISTICAL ANALYSIS 17
RESULTS 18
DISCUSSION 26
CONCLUSIONS 29
CHAPTER 3: METHOD FOR QUANTIFYING COMPLEX PHASE PLANE PORTRAITS 31
ABSTRACT 31
INTRODUCTION 32
PRECEDING METRICS & ALGORITHMS 35
METHODS 37
POLYAREA APPROXIMATION METHOD 37

Inner Loop Identification Scheme 38
Footprint and Convex Hull Data Point Identification 40
Results 42
Comparison of Polyarea and Flood-Fill Computation Methods 43
Comparison of PAR and RED Computation Methods 48
Discussion 48
Conclusions 50
Chapter 4: Quantitative Assessment of Spasticity by Phase Plane Analysis 52
Abstract 52
Introduction 53
Spasticity and Assessment 53
Treatment 54
Methods 55
Subject Pool 55
Study Design 56
Instrumentation and Test Protocol 56
Signal Processing 57
Performance Measure 58
Statistical Analysis: Development of a linear regression model 58
Results 60
Clinical Measures 60
Phase Portraits and Kinematic Data Measures 61
Overview of Mixed-Effect Models 65
Assessment of Parameter Estimates 67
Treatment Effects 69
Discussion 71
Tools for Intra- and Inter-subject Comparison 71
Treatment Effects 72
Pace-dependencies 73
Limitations of Study 75
Conclusions 75
Chapter 5: General Conclusions 77
Limitations 77
Justification of Thesis 78
Recommendations for Future Work 79
References 81

LIST OF TABLES

TABLE 1: OVERVIEW OF ASSESSED FEATURES 15

TABLE 2: PERCENTAGE OF CONTROL, POST-STROKE 22

TABLE 3: SUMMARY OF FEATURE ASSESSMENT 26

TABLE 4: CASES OF PHASE PORTRAIT INNER LOOP IDENTIFICATION 42

TABLE 5: SCENARIOS FOR LARGE POLYAREA-FLOOD-FILL DISCREPANCIES 45

TABLE 6: PARTICIPANT DEMOGRAPHICS 55

TABLE 7: CLINICAL MEASURES 61

TABLE 8: SUMMARY OF FIXED EFFECT SIGNIFICANCE (ALL SUBJECTS) 66

TABLE 9: SUMMARY OF SUBJECT-SPECIFIC RANDOM-SLOPE MODELS (ALL SUBJECTS) 67

TABLE 10: SESSION-SPECIFIC RANDOM-SLOPE MODEL COEFFICIENTS 68

TABLE 11: BY-SUBJECT PERFORMANCE METRIC COMPARISON 70

TABLE 12: MS SUBJECT PERFORMANCE MEASURES PRE-, POST- TREATMENT 70

LIST OF FIGURES

FIGURE 1: MECHANICAL ARM SUPPORT AND TRACKER (MAST) 14
FIGURE 2: IDEAL SHAPES GENERATED BY A SINGLE ELBOW FLEXION 19
FIGURE 3: COMPARISON OF LOCAL EXTREMA AND INNER LOOPS 20
FIGURE 4: DISTRIBUTIONS OF LOCAL EXTREMA COUNT AND INNER LOOP COUNT 22
FIGURE 5: TEMPORAL PROFILES TO AV PORTRAIT 23
FIGURE 6: VISUAL COMPARISON OF KMV AND CM 24
FIGURE 7: AP PHASE PORTRAITS GENERATED BY (A) CONTROL AND (B) STROKE SUBJECTS 25
FIGURE 8: FLOOD-FILL APPROXIMATION METHOD 36
FIGURE 9: DEMONSTRATION OF THE INNER LOOP IDENTIFICATION SCHEME 38
FIGURE 10: INNER LOOP IDENTIFICATION AV PHASE PORTRAITS 39
FIGURE 11: CONVEX HULL OF A COMPLEX AV PHASE PORTRAIT 40
FIGURE 12: FOOTPRINT OF A COMPLEX AV PHASE PORTRAIT 41
FIGURE 13: REPRESENTATION OF THE PAR EQUATION. 42
FIGURE 14: A COMPARISON OF POLYAREA AND FLOOD-FILL METHOD 44
FIGURE 15: PHASE PORTRAIT CASE STUDIES 45
FIGURE 16: COMPARISON OF PREDICTED AREA AND ACTUAL AREA 47
FIGURE 17: COMPARISON OF PAR SCORES WITH RED SCORES. 48
FIGURE 18: OVERVIEW OF DATA COLLECTION TO PHASE PORTRAIT PROCESS 58
FIGURE 19: RESIDUAL PLOTS PRE- AND POST- WEIGHTED VARIANCE FUNCTION. 60
FIGURE 20: AV PHASE PLANE PORTRAITS SHOWING PACE DEPENDENCY 62
FIGURE 21: INTER-SUBJECT COMPARISON OF PAR SCORES. 63
FIGURE 22: LATTICE PLOTS SHOWING THE EFFECT OF TESTING PACE. 64

CHAPTER 1: GENERAL INTRODUCTION

Upper motor neuron syndrome and Spasticity

Brain lesions in upper motor neurons can disrupt signal transmission through one or more of the descending pathways, causing upper motor neuron (UMN) syndrome. Symptoms include spasticity, hypertonia, clonus, a positive Babinski sign, weakness, fatigue, and dexterity loss (Pandyan et al. 2005, Barnes and Johnson 2008). UMN syndrome is common in stroke, multiple sclerosis, cerebral palsy and traumatic brain injury patients. Often, the lesion impairs motor coordination; for instance, a reaching trajectory that once followed a smooth, natural motion along a minimal energy path becomes jerky and unpredictable.

A highly common positive symptom of UMN syndrome is spasticity. Studies have reported that as many as 20 percent of post-stroke patients, 60 percent of multiple sclerosis (MS), 80 percent cerebral palsy, and 75 percent traumatic brain injury patients seek treatment for spasticity (Watkins et al. 2002, Physicians 2009, Koman et al. 2008). Spasticity can impact a number of ordinary activities of daily living (ADL), including eating, washing, and dressing, as well as affect one's ability to work, mood, and motivation. Studies have found that nearly 35 percent of MS patients describe their spasticity severity level among the following categories: 'frequently affecting', 'severely limiting' or 'completely preventing' their ability to complete daily activities (Rizzo et al. 2004). In Sweden, it has been estimated that the costs incurred within the first year post-stroke for an individual with spasticity is four times greater than one without and as much as twenty times greater in the United States (Lundstrom et al. 2010).

Lance described spasticity as a motor disorder characterized by a velocity-dependent increase in resistance during passive movement of a person's limb and is seen in subjects with UMN lesions (Lance 1980). In recent years, many have advocated for better understanding and assessment of spasticity in a clinical setting, as it is frequently used as an "umbrella term" for the positive UMN syndrome symptoms, although Lance's commonly accepted, well-published definition is quite unique and specific (Wood et al. 2005). However, it has since been noted that findings from spasticity-related studies contradict Lance's original definition, and other, less restrictive, definitions may be more appropriate from both a clinical and research-driven standpoint (Malhotra et al. 2009). Advocates pushing for both research advancements in spasticity and improvements in clinical diagnosis and treatment have surfaced with modified definitions, although a consensus has yet to be reached. Groups have proposed spasticity be redefined as, "disordered sensory-motor control, resulting from an upper motor neuron lesion, presenting as intermittent or sustained involuntary activation of muscles" based on a careful examination of literature, in which they concluded that spastic muscle activity does not always present with stretch reflex hyperexcitability nor did the literature support the notion that increased muscle activity always corresponds to increased resistance (Burridge et al. 2005, Pandyan et al. 2005). Additionally, Pandyan, et al. questioned whether velocity-dependence is a characteristic reserved only for spasticity but reasoned that velocity-dependence is a normal viscoelastic property of soft-tissue, therefore finding it inappropriate to make velocity a defining trait (Pandyan et al. 2005). Malhotra's review supports the argument for a modified definition, concluding that the aforementioned definition developed by the SPASM Consortium—an interdisciplinary

team of specialists in spasticity, advocating both clinical and research advancements from 2002 to 2005—and published by Pandyan, Burridge, et al. best represents the current state, in which spasticity is understood. The definition encompasses most positive features of UMN syndrome, and, although vague, it is promoted as being the most clinically relevant definition, while providing researchers the flexibility to approach spasticity from a broad sense and, in time, refine and focus the definition based on their findings. However, it may be argued that Malhotra, et al.'s promotion is biased, as coauthors are serving member of the SPASM Consortium (Malhotra et al. 2009).

Despite disagreement on spasticity's proper definition, it is agreed that spasticity has a neurogenic component, causing overactive muscle contractions, and a biomechanical component, resulting in changes in muscle properties, including stiffness and length. Due to its complexity, spasticity calls for a team of specialists—including neurologists, physical therapists, occupational therapists, and rehabilitation engineers—to decide the best course of treatment (Burridge et al. 2005, Hefter et al. 2012, Foran et al. 2005, Physicians 2009).

Treatment

A variety of treatment options exist to suit the uniqueness of each patient's case. Although it may be decided that some patients need little or no treatment, others require a combination of methods to address symptoms and deter secondary complications. Physical therapy is often needed to improve gross motor function, improve joint range of motion, and discourage muscle contracture, in addition to occupational therapy to focus on improving ADL. Specialty equipment—for example, wheelchairs, gait trainers, orthotics, and casts—may also be needed to encourage mobility and improve

functionality (Bandi and Ward 2010). Medications, such as baclofen, may also be administered, either orally or intrathecally, to inhibit excitation and ease muscle contraction. In addition, some find botulinum toxin injections (BTI) beneficial in discouraging muscle hyperactivity—though the effects gradually abate—while others argue that BTI does not significantly improve function (Bensmail et al. 2010, Physicians 2009, Hefter et al. 2012).

Assessment

Standard methods for assessing a patient's level of spasticity are based on qualitative observations, and currently, there are no reliable, quantitative methods for assessing spasticity. The Ashworth and Modified Ashworth scale (MAS) are based on the perceived resistance to stretch when an affected limb is passively moved. Both tests assign a subjective rating—on a scale from 0 to 4—to the severity of spasticity; however, the modified-version incorporates an extra level in the scale to distinguish mild from moderate spasticity (Bandi and Ward 2010, Bohannon and Smith 1987). In 2008, Alibiglou, et al. studied the neural and muscular components of joint stiffness; results from this study failed to correlate with assigned (modified) Ashworth scores, and others have urged physicians to discontinue use (Alibiglou et al. 2008, Fleuren et al. 2010). Likewise, the Tardieu Scale is based on a 5-point system and is used during passive limb movement; for this test, the examiner is concerned with the angle at which the spastic event, or "catch", occurs over test variations (slow speed, fast speed, and with gravity) (Bandi and Ward 2010). Due to the test's subjective nature, it has been reported that the experience of the examiner limits the reliability of the Tardieu Scale (Ansari et al. 2008).

Although there is a call for methods that quantify one's spastic severity, a reliable, well accepted system has yet to be implemented.

In accordance to Lance's definition, in a clinical setting, spasticity is typically assessed by a therapist while *passively* moving a subject's limb, and there are a limited number of research studies that have investigated active motion test protocols. However, Burridge, et al. have voiced the importance of considering both passive and active movements to fully grasp how neurogenic features differ from mechanic; their belief is that an active test protocol may yield a more valuable and realistic assessment of a patient's condition (Burridge et al. 2005). Further discussed by Van der Krogt, et al., active test protocols provide insight into the neurogenic aspects, yielding information about voluntary muscle properties, whereas passive protocols highlight biomechanical aspects, such as tissue and joint stiffness properties (van der Krogt et al. 2012).

Previous studies based trajectory analysis on the minimization of a single cost function (i.e. avoiding obstacles, jerk), while other found it more appropriate to base their analysis on a combination of cost functions (Wininger, Kim, and Craelius 2009, Berret et al. 2011); however, there is no consensus on what is the most appropriate approach. Commonly, impairments change the trajectory's behavior from one that is smooth to one that is complex and unpredictable, yet the degree of complexity may fall along a spectrum and deciding to classify a motion as smooth or unsmooth is simply not "black or white." Here, I will discuss a graphical method and present a measure, which together are capable of qualitatively and quantitatively characterizing smoothness, use these as a means of exploring motor complexities, and aim to understand its many shades.

Statement of Need

The qualitative assessment of spasticity is a major limitation on progress in understanding and treating the syndrome (Rekand 2010, Ansari et al. 2008). An evaluation of a patient's condition that is based on subjectivity results in inconsistent assessments, as well as discrepancies across therapists, affects the therapy protocol and inaccurately tracks progression.

In order to best assess a patient's condition and uniquely tailor treatment plans, diagnostic tests used to assess spastic severity in subjects are in need of the following:

1. A standardized protocol that assesses a patient's degree of spasticity, incorporating both standardized quantitative assessments and qualitative, subjective assessment to properly track a patient's progression though treatment (intra-subject comparison), as well as the ability to draw inter-subject comparisons.
2. A protocol that improves intra-physician and inter-physician accuracy of assigning a patient to the most appropriate severity level.
3. The ability to gauge dose and duration of pharmaceutical interventions with guidance from both quantitative and qualitative test results.

Hypotheses

The present work aims to improve the quality of care of patients suffering from spasticity, through the development of reliable metrics that will assist a provider with diagnosis and designing a treatment plan. It has been shown that human movement is accomplished by nonlinear processes whose behavior can be visualized and quantified in phase space. Specifically, I will test the hypothesis that the efficiency of single-joint

movements can be quantified by dynamical analysis, including kinematical phase portraits. The investigation progressed through three main hypotheses.

Hypothesis 1:

Phase portraits accentuate aberrant, unsmooth movements that are not discernible in the temporal domain by providing an easily recognizable geometric form with normal movement and deviations from this form with impaired movement. Additionally, phase planes will provide a visual and quantifiable record for assessing performance across multiple test sessions and simplify intra-subject and inter-subject comparisons, exposing behavior obscured by temporal plots.

Hypothesis 2:

Phase Area Ratio (PAR) scores appropriately represent the complexity of a movement's profile and provide insight otherwise lost by conventional methods.

Hypothesis 3:

Quantification of spasticity is possible through the use of temporal graphs, phase portraits, and additional metrics of smoothness. These may not correlate well with established, qualitative and quantitative methods, but may correlate with certain treatments.

Thesis Overview

Here, objective measures of complex movement are presented and compared, in hopes that they may be used to quantify and report symptoms, such as spasticity. In Chapter 2 of this thesis, kinematic data gathered from both stroke and control subjects are

used to investigate what can be learned about one's level of impairment by viewing the data in phase space as compared to the temporal frame. Through this first segment, it is shown that phase portraits are a useful tool to display kinematic motion and yield features that distinguish impaired movement. This leads to the research focus presented in Chapter 3—quantification of a phase portrait trajectory. A novel scheme, based on computational geometry, for quantifying the area within a phase portrait is presented and compared with previously developed methods (Atler et al. 2015). Each of these area finding methods may be used to compute the Phase Area Ratio (PAR)—a metric, which will promote inter- and intra-rater reliability, allow therapists to easily track a patient's progression across trials, and validate the efficacy of a treatment protocol. Chapter 4 demonstrates use of the PAR metric to track multi-month progression of subjects suffering from Secondary Progressive Multiple Sclerosis (SPMS) and receiving anti-spasticity drug treatment. Additionally, it is shown that, through use of this metric, it is possible to draw inter-and intra-subject comparisons and study such things as pace-dependencies and limb differences.

CHAPTER 2: HUMAN MOTION ANALYSIS USING SPATIO-TEMPORAL REPRESENTATION

Abstract

Objective: The objective of this study was to compare temporal and phase plane domains as metrics of human motion smoothness. *Method*: Subjects with UL impairment due to stroke (N = 6, 5 M/1F) and control subjects (N = 3, 2M/1F) performed single-joint extension-flexions at the elbow using the Mechanical Arm and Support Tracker (MAST). Processed data were plotted in the temporal frame and as phase portraits and assessed for features believed to indicate atypical behavior—excessive local extrema (E), kinematic mean variation (KMV), inner looping (L), centroid drift (CD), and stiffness. *Results*: A total of 302 extension-flexion repetitions (166 post-stroke/136 control) were displayed as temporal plots and phase portraits. Local extrema event rate were two times greater among post-stroke subjects than control subjects ($p < 0.0001$); repetitions with excessive local extrema were nearly always generated by post-stroke subjects (96-, 89-, and 95 percent of *p-t*, *v-t*, and *a-t* plots). Similarly, the inner loop event rate was more than three times greater for post-stroke subjects than control subjects ($p < 0.0001$), accounting for 97- and 95 percent of the total VP and AV phase portraits with inner loops. Inter-repetition variation, measured by centroid movement and kinematic mean variation, between post-stroke and control was significant in both graphing schemes ($p < 0.001$ for all cases). Stiffness values were found to be greater in control subjects than in imparied subject ($p = 1$), due to the nonlinear nature of the AP phase portraits. *Conclusions*: A quantification scheme that incorporates alternative ways to display movement data other than conventional temporal graphs may be useful in assessing atypical movement. It is

recommended that future work focuses on development and implementation of said scheme.

Introduction

Nearly 800,000 Americans experience stroke each year (Go et al. 2014). Post-stroke residual effects are highly common, with more than 50 percent experiencing a motor disability and over 40 percent developing spasticity in an upper or lower extremity (Go et al. 2014, Urban et al. 2010, Winstein et al. 2003). The direct and indirect cost associated with post-stroke treatment has been estimated at $36.5 million per year and may include a team of specialists and a combination of physical, occupational and speech therapy, medications, orthotic intervention, as well as many additional services (Go et al. 2014).

Previous studies have drawn attention to spasticity assessment and have noted that evaluating a patient's severity level and thus tracking a treatment's efficacy, in order to justify different treatment options and their associated costs, is often based on a provider's subjective assessment (Pandyan et al. 1999, Pandyan et al. 2005). However, potential risks may arise when a treatment plan, i.e. medication dosage, is based on subjectivity (Krach 2001, Smith et al. 1991). There is a need for a standardized measure that quantifies extremity motor patterns, allowing providers to objectively assess the severity of impaired movement, monitor a patient's progress, and validate a treatment's efficacy (Pandyan et al. 1999, Pandyan et al. 2005).

The trajectory path of single-joint extension-flexion is commonly shown using temporal plots, in which position, velocity, or acceleration is dependent on time. Previous studies have explored features to describe a motion trajectory, focusing on

kinematic features, including ‘movement time,’ ‘peak velocity,’ and ‘number of movement units’ or ‘submovements’ (Chang et al. 2008, Alt Murphy, Willen, and Sunnerhagen 2011, Rohrer et al. 2002, Rohrer et al. 2004). ‘Submovements,’ which are essentially subsequent, discrete Gaussian curves that become blended into one as the fluidity of a motion improves, are promoted as a measure of ‘smoothness.’ Assessing stroke patients before and after one year of treatment, Rohrer, et. al. found that post-treatment ‘submovements’ peaked at a higher velocity, stretched over a longer duration, and had greater overlap, so fewer ‘submovements’ were needed to complete a given task (Rohrer et al. 2002, Rohrer et al. 2004).

Likewise, in this study, certain features were extracted from the temporal plots. The present study considers a feature related to ‘movement units’ and anticipates findings similar to prior publications: position, velocity and acceleration profiles generated by impaired subjects will fluctuate more than the profiles generated by a non-impaired subject.

However, we are faced with the question: is it possible to pair a qualitative description of the level of impairment, in a manner that is easily communicated, providing a visual image, across various disciplines (engineers, neurologists, physical therapists, etc.) with a quantitative measure? The dialogue becomes complicated, in that the ideal shapes of temporal graphs (sigmoidal for position-time; Gaussian for velocity-time; sinusoidal for acceleration-time) are less impressionable than a basic geometric shape. Thus, variations in the ideal shape are more difficult to qualitatively describe.

Alternatively, the data may be viewed in the phase plane, in which the aspect of time is removed and data is plotted with one kinematic feature against another (i.e. a state

variable against its first or second derivative with respect to time), to form a distinct shape. It is hypothesized that velocity-position (VP) and acceleration-velocity (AV) phase portraits generated from the movement of healthy individuals will be smooth, elliptical and near symmetrical, whereas portraits from impaired movement will show asymmetrical irregularities, including inner loops and concavities.

Acceleration-position (AP) phase portraits provide insight into linear and nonlinear motor behavior. With acceleration directly proportional to force, a subject that moves with ease through the extension/flexion cyclical motion will generate a AP portrait that is either linear or with a linear region (Guiard 1993). It is hypothesized that slope of the linear region coincides with stiffness, as it is expected that a subject exhibiting impairment will yield an AP portrait of greater slope—and, therefore, indicates an increase in stiffness—than one exhibiting smooth motion.

In this study, we examined qualitative and quantitative features that describe the shape of temporal plots and phase portraits and compared how time-based and phase-based plotting schemes identify typical motion from complex kinematic data. The goal of this study was to better understand the features from each plotting method that provide different insights into motor behavior and may be used in future studies to develop a standardized scheme for quantifying movement complexity. We hypothesized that spatio-temporal features are affected by complex motion and therefore, graphing tools may be useful for:

1. Capturing a visual record of a subject's performance that may be used to draw comparisons within and across subjects.

2. Identifying graphing features that may differentiate impaired from typical movement.

The present study aims to show that plotting methods offer a tool to describe movement performance and graphical features will deviate from a predefined ideal in the presence of impaired motion.

Methods

Subject Pool

Six post-stroke subjects (5 male, 1 female) and three control subjects (2 male; 1 female) participated in this study. All participants were over the age of 18 years and with no known cognitive impairments that would inhibit compliance with the research protocol or the ability to provide informed consent. Approval for subject testing was granted by Rutgers IRB.

Instrumentation and Test Protocol

Subjects were seated and arms were comfortably secured in the Mechanical Arm and Support Tracker (MAST) (Wininger, Kim, and Craelius 2009). The MAST allowed a subject to perform single-joint extensions and flexions about the elbow along the horizontal plane, free from gravitational influence. Data were collected from the MAST's potentiometric goniometer and accelerometer (ADXL330) via a LabVIEW (NI Instruments) graphical user interface (GUI), while the subjects participated in both frequency-specific, tracking tasks and self-paced tasks.

Figure 1: Mechanical Arm Support and Tracker (MAST)

Signal Processing

Velocity data were computed by numerical differentiation of the position data gathered by the goniometer. A locally weighted regression (LOESS) approach, with a five percent window size, was used to smooth the position, velocity, and acceleration data. To adjust for amplitude differences, the data-series were normalized to a scale of 0 to 1.

Repetitions (flexion-extension combinations) from each trial were identified and separated via an automated Matlab (The Mathworks, Inc.) program, using angular threshold filtering. After visual inspection of a subject's sequence of repetitions, threshold values were adjusted, as needed. Repetitions were further divided into an extension and flexion, as determined by the repetition mid-point.

Temporal & Phase Plot Feature Assessment

Processed data were translated and plotted in the temporal frame and as phase portraits. The majority of the graphing techniques used in this study were performed

using the complete repetition (flexion-extension), with the exception of the AP phase portrait, in which each portrait represented a single extension or flexion.

The temporal plots and phase portraits were visually inspected and algorithmically assessed for features listed in Table 1. These features were specifically chosen because they provided a visual cue that motion deviated from expected motion, applied to both domains, and can be associated with physical parameters.

Table 1: Overview of Assessed Features

Feature	**Domain**	**Description**
Local Extrema	Time (*p-*, *v-*, *a-t*)	Identified as the point where a function's first derivate changes from positive to negative, or vice versa. Expected Values: $E_p = 1$; $E_v = 2$; $E_a = 4$ or 5
Inner Loops	Phase plane (*VP, AV*)	Identified as a minimum of eight data points forming a complete loop within the convex hull of a phase portrait. Expected Values: $L_{VP} = 0$; $L_{AV} = 0$
Kinematic Mean Variation	Time (*p-*, *v-*, *a-t*)	Measured as the Euclidean distance between the mean value of two consecutive temporal graphs. Expected Values: $KMV_p \approx 0$; $KMV_v \approx 0$; $KMV_a \approx 0$
Centroid Movement	Phase plane (*VP , AV*)	Measured as the Euclidean distance between the centroids of two consecutive phase portraits. Expected Values: $CM_{VP} \approx 0$; $CM_{AV} \approx 0$;
Stiffness	Phase plane (*AP*)	Related (i.e. directly proportional) to the slope of AP phase portrait. Expected Value: $k \propto \ddot{\theta}/_{\theta}$

Feature Definitions

Local extrema (Ei), where i = p, v or a, for position, velocity or acceleration, respectively. A local extrema is identified as the point at which the function's first derivative changes from positive to negative slope, or vice versa. It is expected that typical motion of an extension-flexion trajectory (*single repetition*) yields 1, 2, or 4-5 local extrema in position-time, velocity-time, or acceleration-time graphs, respectively. Identification of local extrema exceeding these amounts may indicate atypical or complex motion.

Inner loops (Lj), where j = VP or AV, for velocity-position or acceleration-velocity phase portraits, respectively. It is expected that typical motion of an extension-flexion trajectory yields velocity-position and acceleration-velocity phase portraits that are near elliptical and free of points within the convex hull. A phase portrait with points existing within its convex hull, such as points forming inner loops, may indicate atypical or complex motion. A sequence of points constituted an inner loop if it included at least eight data points. This method considered only whether an inner loop existed within the phase portrait and did not consider the effects of large verses small loops.

Kinematic Mean Variations (KMVi), where i = p, v or a, for position, velocity or acceleration, respectively, is defined as the Euclidean distance between the mean value of two consecutive temporal graphs. Synonymous to centroid movement (CM), it is expected that consecutive repetitions of typical arm extension-flexion trajectory yield temporal graphs with minimal variation in kinematic mean, and significant variation between consecutive temporal graphs may indicate atypical movement.

Centroid Movement (CMj), where j = VP or AV, for velocity-position or acceleration-velocity phase portraits, respectively, is defined as the Euclidean distance between the centroids of two consecutive phase portraits. DiBerardino, et. al. demonstrated that the shift in consecutive phase portraits' centroids may provide insight into inter-stride variability during gait and may be useful for quantifying the performance of a limb's trajectory (DiBerardino et al. 2010). Herein, it is expected that consecutive repetitions of typical arm extension-flexion trajectory yield phase portraits with minimal centroid movement, and significant centroid movement between consecutive phase portraits may indicate atypical movement.

Stiffness (k), as measured from the acceleration-position phase portrait. Typical motion is also expected to yield an acceleration-position phase portrait with a distinct linear region, whereas complex motion may produce a phase portrait void of a linear region. The slope of the linear region coincides with stiffness, so it is anticipated that the slope of linear region will increase with an individual's impairment level. Elbow joint stiffness may be represented by the following equation:

$$Stiffness, \qquad k \propto \frac{\ddot{\theta}}{\theta} \tag{1}$$

where $\ddot{\theta}$ = angular acceleration and θ = angular position of elbow.

Feature Assessment and Statistical Analysis

Histograms of the number of local extrema (E_p, E_v, E_a) in position-time, velocity-time, and acceleration-time graphs, and the number of inner loops (L_{VP}, L_{AV}) in velocity-position and acceleration-velocity phase portraits were approximated by a Poisson

distribution. The ratio of the post-stroke to control subject Poisson rates was tested using an exact conditional test (C-test), as developed by Przyborowski and Wilenski and was implemented in R (Team 2013, Przyborowski and Wilenski 1940).

Centroid drift (CD) value histograms were right-skewed and best fit by a lognormal distribution. CD values were compared between the post-stroke and control subject groups using Wilcoxon Rank Sum test. Wilcoxon Rank Sum test is a nonparametric test and, therefore, makes no assumptions, regarding the probability distribution of a data set (Wilcoxon 1945). Also, the Wilcoxon Rank Sum test is adept to handle repeated measures, as is the case at hand with multiple repetitions from subjects over several test sessions.

Kinematic mean variation (KMV) value histograms were also right-skewed and best fit by a lognormal distribution. Similar to CD, KMV values were compared between the post-stroke and control subject groups using Wilcoxon Rank Sum test. Results generated from these approximations are further discussed in the following section.

Results

In this study, 302 repetitions (flexion-extension) were analyzed and displayed as temporal and phase portraits. Through visual and algorithmic inspections, these plots were closely examined (166 repetitions from post-stroke subjects and 136 repetitions from control subjects) for the features previously discussed.

Using the data presented here, a full repetition (i.e. a concatenated extension-flexion sequence) was needed to form a complete ellipse. Figure 2 (a-c) provides examples of typical time-based curves for unimpaired single-joint flexions at the elbow,

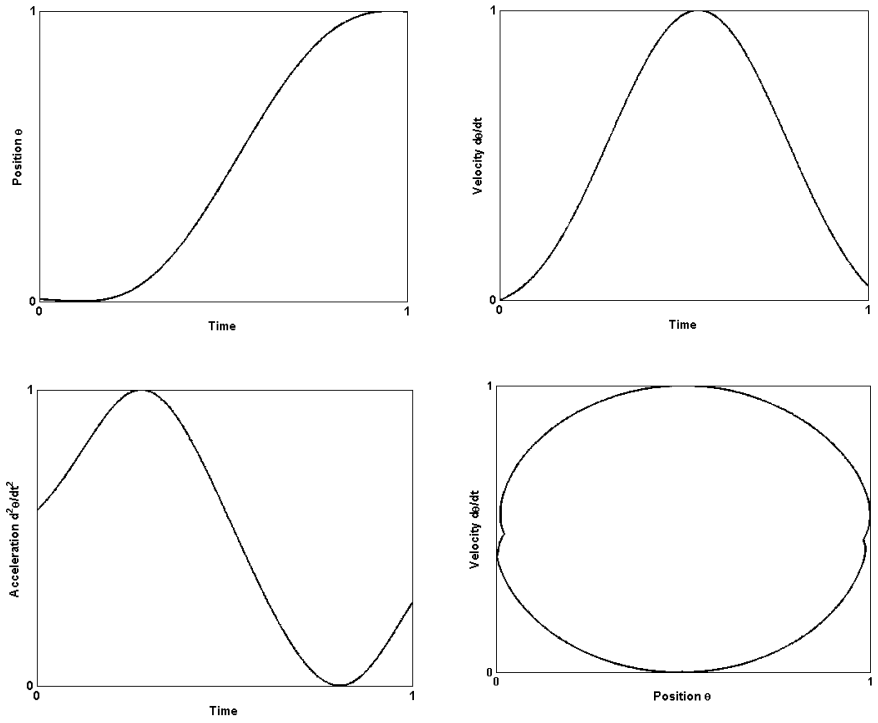

Figure 2: Ideal shapes generated by a single elbow flexion: (a) sigmoidal for p-t; (b) Gaussian for v-t; (c) sinusoidal for a-t. (d) elliptical VP phase portrait

and the fourth plot, Figure 2 (d), demonstrates the ideal phase portrait—shown here as VP, although an AV portrait yields similar results.

Figure 3 depicts a comparison of temporal and phase plots generated by a control (Figure 3 *left column*) and stroke subject (Figure 3 *right column*) and highlights two of the features examined in this study—local extrema and inner loops. For clarity, we selected a single repetition each from a control and stroke subject. The temporal plots (Figure 3 a-b) and phase portraits (Figure 3 c-d) show noticeable differences, as highlighted in red. In a single extension-flexion repetition, the control subject yields a position-time plot that follows the shape of Gaussian curve (R^2 = 0.94), and thus, yields the expected number of local extrema (E_p = 1; E_v = 2). On the contrary, the stroke subject's position-time plot does not follow the expected Gaussian shape (best-fit

Gaussian, R^2 = 0.13) and yields excessive local extrema (E_p = 3; E_v = 4). Additionally, an inner loop is present in the stroke subject's phase portrait (L_{VP} = 1) and not in the control's (L_{VP}= 0).

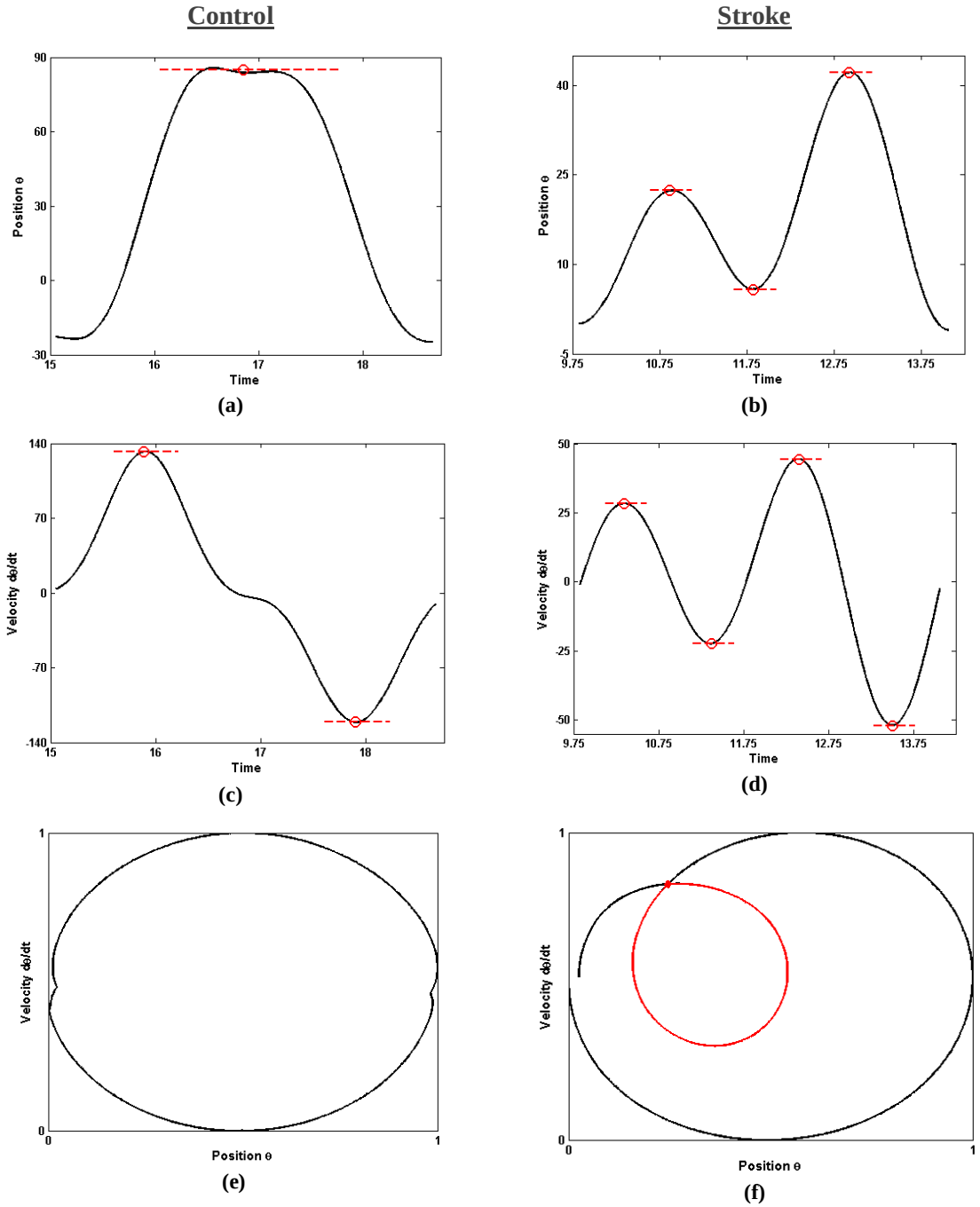

Figure 3: Comparison of temporal plots with marked local extrema and phase portraits with marked inner loops generated by control subjects (*left column*) and stroke subjects (*right column*). All figures were generated using a complete extension-flexion repetition. (a)-(b) Position-time graphs (*control:* E_p = 1; *stroke:* E_p = 3); (c)-(d) velocity-time graphs (*control:* E_v = 2; *stroke:* E_v = 4); (e)-(f) Velocity-position phase portraits (*control:* L_{VP} = 0; *stroke:* L_{VP} = 1)

Local Extrema Count

Comparison of local extrema count between control and post-stroke subjects revealed a significant difference in performance, with the local extrema event rate of post-stroke subjects being more than two times greater than that of the control group ($p < 0.0001$). Considering all repetitions, a total of 24 position-, 54 velocity-, and 41 acceleration verses time plots were identified as having an excessive number of local extrema (greater than 1, 2, and 5 extrema, respectively). Of those identified with excessive extrema, nearly all repetitions (96-, 89-, and 95 percent of *p-t*, *v-t*, and *a-t* plots) were generated by post-stroke subjects. Within the post-stroke group, 14-, 29-, and 23 percent of the repetitions yielded temporal plots (p-t, v-t, a-t, respectively) with excessive extrema, whereas far fewer cases with excessive fluctuations were identified in the control group (0.74-, 4.4-, and 1.5 percent of control subject generated *p-t*, *v-t*, and *a-t* plots). Results are summarized in Table 2.

Inner Loop Count

Similarly, summarized in Table 2, a comparison of inner loop count between the two groups also showed a significant performance difference, with the inner loop event rate of post-stroke subjects being more than three times greater than that of the control group ($p < 0.0001$). Of the 302 repetitions generated by post-stroke and control subjects, at least one inner loop occurred in 11 percent of VP phase portraits and 17 percent of AV phase portrait. Post-stroke subjects' single joint trajectories (166 repetitions) accounted for 97 percent of the total VP phase portrait inner loops and 95 percent of the total AV inner loops. Within the post-stroke group, 19 percent of the repetitions yielded VP phase

Table 2: Percentage of Control, Post-stroke Repetitions Exceeding Typical Movement Expectations

	Local Extrema (E_i)			Inner loops (L_j)	
	E_p (>1)	E_v (>2)	E_a (>5)	L_{VP} (>1)	L_{AV} (>1)
Control (%)	0.74	4.4	1.5	0.74	3.6
Post-Stroke (%)	14	29	23	19	27

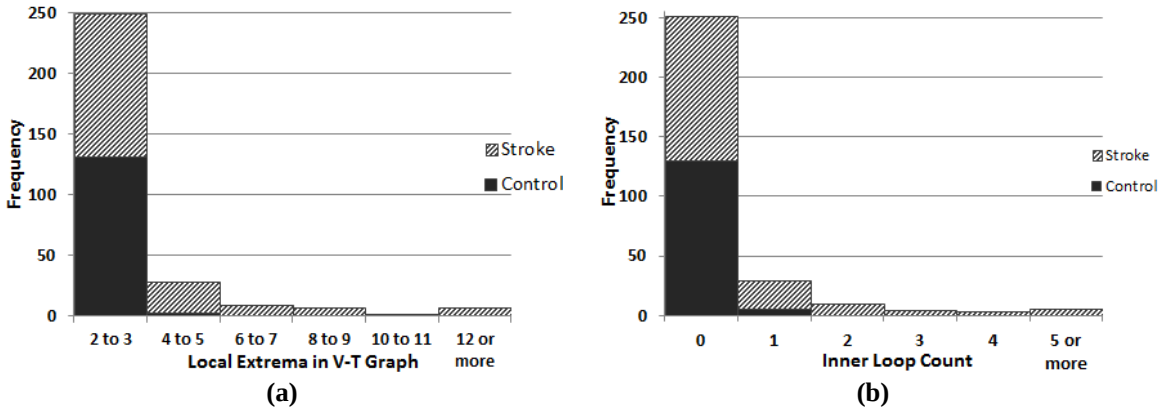

Figure 4: Distributions of (a) local extrema count in velocity-time graphs and (b) inner loop count in AV portraits

portraits with a minimum of one inner loop, and 27 percent yielded AV phase portraits with a minimum of one inner loop. Far fewer portraits with inner loops were identified in the control group (0.74 and 3.6 percent of control subject generated VP and AV phase portraits). Additionally, with post-stroke subjects, it was common for phase portraits to exhibit greater than one inner loop per repetition's phase portrait (31 and 47 percent for VP and AV phase portraits, respectively).

Overview of Counting Features

As shown in Table 2 and Figure 4, the count of local extrema and inner loops yielded similar results due to the fact that they are related: fluctuations in temporal profiles may lead to an inner loop when the variables are paired and plotted in phase-

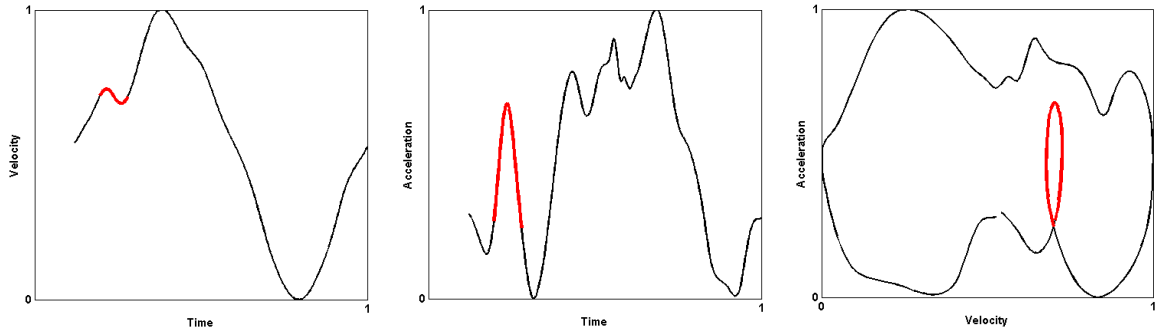

Figure 5: Fluctuations in temporal profiles coincide with inner loop in AV portrait

space (Figure 5). Discussed later in more detail, temporal profiles were of a less impressionable, ideal form and the subtle variations led to many erroneous computer-generated results and required assessment by visual inspection. Phase portraits, on the other hand, had a distinct geometric, ideal form, which made kinematic deviations more pronounced and easy to visually and algorithmically inspect.

Centroid Movement (CM) and Kinematic Mean Variation

Figure 6 demonstrates the assessment of Centroid Movement (CM) and Kinematic Mean Variation (KMV) values. The temporal and phase plots generated by a control (Figure 6 *left column*) and stroke subject (Figure 6 *right column*) show two consecutive repetitions; the first repetition (plotted as a gray, broken line) is distinguishable from the second repetition (plotted as a black, solid line) in order to show the variation between repetitions.

A comparison of the distribution of the CM values found a significant difference between the stroke and control subjects for both VP and AV phase portraits (CM_{VP}: $W = 12753$, $p < 0.0001$; CM_{AV}: $W = 12863$, $p < 0.0001$). Likewise, the distributions of KMV values were significantly different between groups for all types of temporal plots (KMV_p:

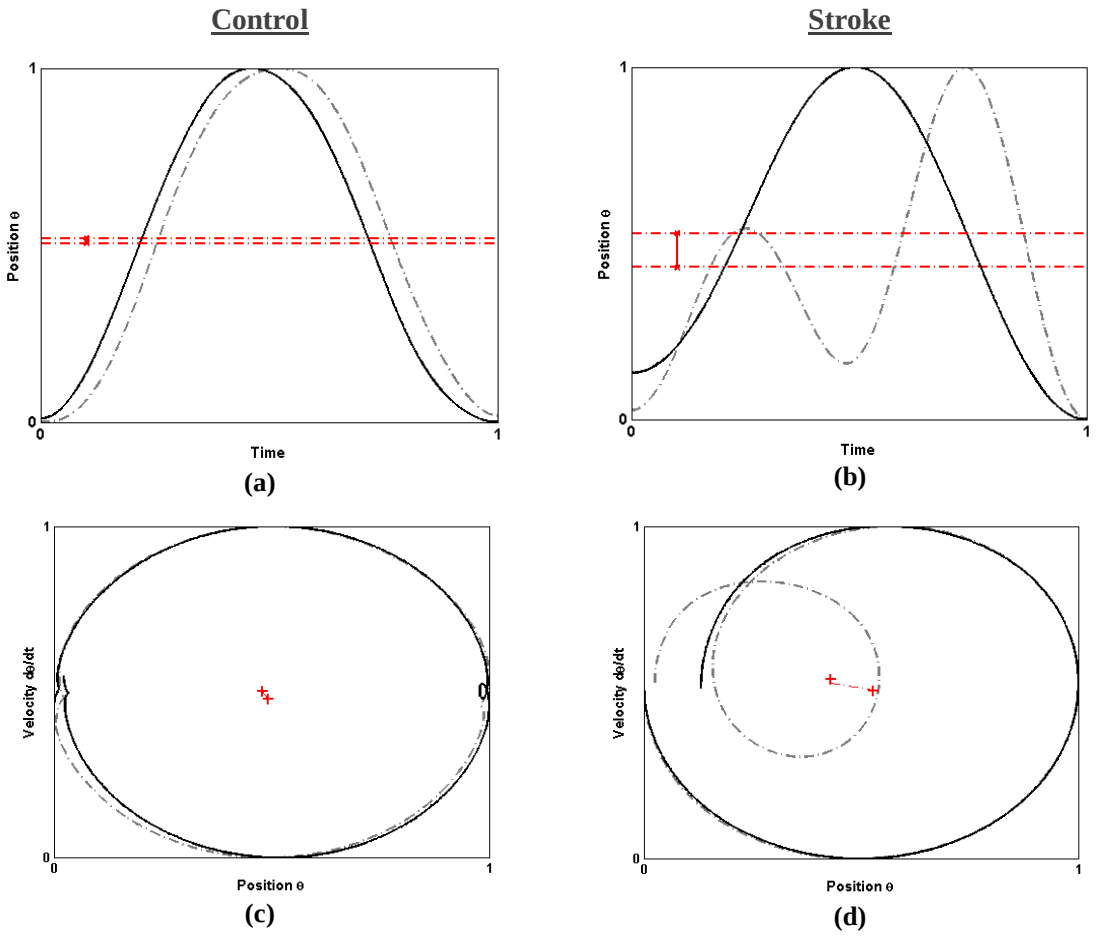

Figure 6: Visual comparison of KMV (a)-(b) and CM (c)-(d) differences between control subjects (*left column*) and stroke subjects (*right column*). Each plot (a)-(d) shows two consecutive repetitions generated by the subject; the first repetition (gray, broken line) is distinguishable from the second repetition (black, solid line)

W = 11577, p < 0.0001; KMV_v: W = 12495, p < 0.0001; KMV_a: W = 11448, p = 0.0002). A complete summary of results is found in Table 3.

Examples of AP phase portraits generated from control and stroke subjects are shown in Figure 7. A linear regression line was fit between the minimum and maximum values, and as mentioned previously, the magnitude of the slope of this line coincides with stiffness. The hypothesis that stiffness, ***k***, increases with an individual's impairment did not hold (t = 4.53, p = 1), and rather, stiffness values were significantly greater in the control group. A distinct linear region was seen in nearly all phase portraits generated by the control group, yet this was often not the case with the stroke subjects. This can be

attributed to the fact that as motion becomes more complex, the AP phase portrait becomes nonlinear. Attempting to fit a nonlinear curve with linear regression results in an unreasonable fit of the data, due to data points deviating far below or far above the best fit line (large negative and positive residuals). Therefore, a more appropriate distinction between a typical and atypical AP phase portrait is to compare the coefficient of determination, R^2, between groups; this measure provides insight into how well a regression line represents the true data. The hypothesis was reformulated:

> *It is anticipated that the coefficient of determination, R^2—measuring how well a regression line represents the expected linear region of an AP phase portrait—is indirectly proportional to an individual's impairment level.*

A comparison of the R^2 values for the stroke and control cohorts indicated that a linear regression line was less representative of an AP phase portrait generated by an impaired subject than by a control subject ($t = 6.93$, $p < 0.0001$).

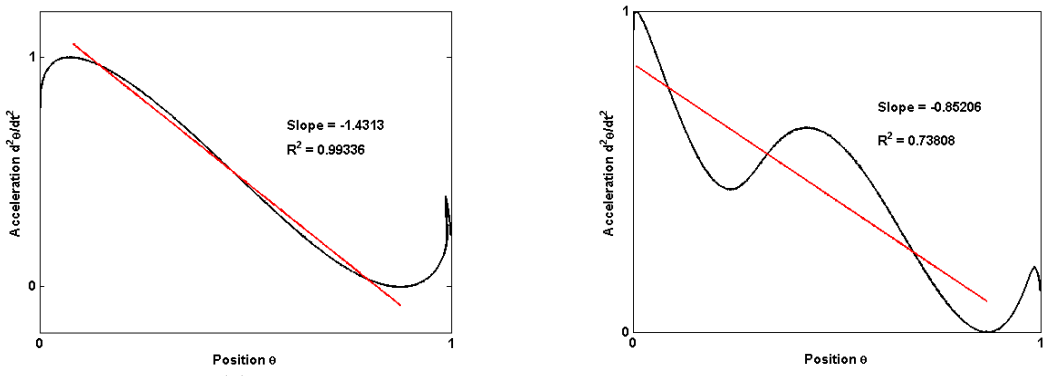

(a) **(b)**

Figure 7: AP phase portraits generated by (a) control and (b) stroke subjects. A linear regression line was fit between the minimum and maximum values, as shown in red.

Table 3: Summary of Feature Assessment

Measure	Subscript	Control	Stroke
Extrema, E_i*	*P*	1.0 (1.0)	1.4 (1.2)
	V	2.1 (1.4)	3.4 (1.8)
	A	2.1 (1.4)	4.8 (2.2)
Loops, L_j*	*VP*	0.015 (0.12)	0.28 (0.53)
	AV	0.05 (0.23)	0.60 (0.78)
Stiffness, *k**	-	1.0 (0.16)	0.98 (0.21)
Kinematic Mean Variation , KMV_i**	*P*	0.020 [0.0000064, 0.21]	0.035 [0.00096, 0.37]
	V	0.021 [0.00054, 0.14]	0.044 [0.000039, 0.39]
	A	0.033 [0.000051, 0.20]	0.053 [0.00029, 0.40]
Centroid Drift, CD_j**	*VP*	0.034 [0.0042, 0.22]	0.074 [0.0051, 0.42]
	AP	0.043 [0.00070, 0.21]	0.081 [0.0052, 0.44]

*Reporting Mean (SD) values for Poisson- and normal-distributed data
**Reporting Median [min max] values for lognormal-distributed data

Discussion

This study tested the hypothesis that movement impairment can be qualitatively and quantitatively assessed using several plotting schemes. Both the conventional approach to view movement kinematics with respect to time and the alternative approach of viewing the time-evolution of two state variables depicted both qualitative and quantitative discrepancies between post-stroke and control subjects. Our analysis focused on answering whether the alternative, phase space method is more capable of distinguishing complex, atypical motion than the conventional temporal method, and we sought to understand the benefits of viewing data in the phase domain.

We analyzed 302 extension-flexion repetitions (166 post-stroke; 136 control) and focused on five main features: *local extrema*, *inner loops*, *kinematic mean variation*, *centroid movement*, and *stiffness*. We emphasized the first two features, as opposed to features, such as peak velocity, time to peak, duration, etc., due to the nature of the

testing protocol. Also, *local extrema* and *inner loops* were both considered to be "visual features" that can be relatively easy to identify and qualitatively compared without computer assistance.

Through this study, it was realized that, in general, temporal profiles were of a less impressionable, ideal form and, at times, fluctuations in a temporal profile were subtle, making qualitative comparisons difficult for an untrained eye. Phase portraits, on the other hand, had a distinct geometric, ideal form, which made kinematic deviations more pronounced. To all those viewing a phase portrait, including researchers, clinicians and patients, deviations from an ideal motor performance, is readily seen. It is anticipated that these graphs may aid in inter- and intra-subject comparisons and provide a useful tool to track patient progression (or regression) and validate therapy protocols.

Quantitative, computer-aided assessments were also performed to further compare the graphing techniques. Under the testing protocol, in which motion is constrained to a single joint, we found that the cases, where an excessive number of local extrema appeared in the temporal graph, were nearly always generated by post-stroke subjects (96, 89, and 95 percent of *p-t*, *v-t*, and *a-t* plots, respectively). The mean number of local extrema in the acceleration-time graphs (average E_a) was less than expected, as some subjects—both control and post-stroke—produced a trajectory with fewer extrema than anticipated for an ideal motion (expected E_a = 4 to 5 extrema in a single extension-flexion, as shown in Table 3. This may be accredited to the subject's motion, but it is more likely a result of algorithmic or human error during the analysis process and is a red flag that limitations exist with temporal graph analysis; most *a-t* profiles generated highly

erroneous computer-generated results and required assessment by visual inspection, which is prone to error.

Likewise, instances of inner loops within a phase portrait were relatively common with post-stroke patients (nearly 20 percent of VP portraits and 30 percent of AP portraits) and were rare occurrences among the control group (1 percent and 4 percent, respectively). This study focused on whether or not a single loop existed within the inner space and did not give consideration to the significance of multiple loops and their relationship to a complexity scale, although it is known that 30 percent and 45 percent of post-stroke, inner-loop-identified VP and AV phase portraits had multiple inner loops. The present findings support the hypothesis that inner loops are an indication of impaired motion. It should also be noted that many portraits did not form a complete, self-intersecting inner loop, but instead, the data formed a concavity within the portrait's convex hull; although an irregular feature, the inner concavity was not included in this particular study. Further studies should focus on the meaning of multiple loops and inner concavities in terms of complexity, energy conservation/dissipation, etc. and how this information may be incorporated into a quantification scheme.

Another interesting finding from this study was that not every post-stroke subject produced visual aberrations in each, or even any, repetitions, and one is left to question whether or not the remaining repetitions would be deemed "atypical" if the feature set was expanded. Although shown to occur at higher rate in stroke subjects than in control subjects, local extrema and inner loops may not be principal features for diagnostic purposes.

In both the temporal and phase domains, the synonymous features of *kinematic mean variation* and *centroid movement* were significantly different between subject groups for both VP and AV phase portraits, and one method was not proven to be favorable over another. Both features have the ability to quantify, what is known as, motor variability, which is based on the premise that, given multiple attempts to complete a given motor task, each repetition will be performed with slight differences in the kinematic profile (Bernstein 1967, Latash, Scholz, and Schoner 2002). Therefore, inter-repetition variation is expected for all motion types (healthy or impaired). However, some symptoms of neurological disorders, such as spasticity, may be triggered inconsistently, and so high inter-repetition variation may support a diagnosis and improved inter-repetition variation may justify an effective treatment protocol.

Stiffness was greater in control subjects than impaired individuals ($p = 1$), which was not anticipated. It was confirmed, however, that stroke subjects generated AP portraits that often lacked a linear mid-region, a common attribute seen with the control group, and therefore, a linear regression line was less representative of an AP portrait generated by an impaired subject than by a control subject ($p < 0.0001$). It is concluded that a nonlinear AP portrait may not provide an accurate representation of a patient's physical joint attributes, although this may be possible when a linear region is present.

Conclusions

When evaluating movement complexity, spatio-temporal graphing methods reveal various features that may be used to qualitatively and quantitatively describe motion. These features are beneficial, since they draw distinctions between healthy and impaired motion. From this work, it was shown that phase portraits are a useful tool to display

movement data, retain features that distinguish impaired movement, while providing a distinct visual record for quick comparison.

Limitations exist within the present work; the study was concerned with identifying features and verifying that, based on the feature, a population of stroke subjects performed single-joint movement significantly different from a controlled population. The study was unconcerned with answering how the feature varied across levels of impairment and whether the particular feature may be used to classify a motion as a specific type. This leads to a question that may be explored in future work: have we identified principal features that may be used for diagnostic purposes (healthy *vs.* impaired) or distinguish degrees of impairment?

Additionally, the examination of phase portraits was limited and only "scratched the surface" of their potential as a diagnostic tool. The method used here to identify an inner loop was only concerned with whether a single loop existed and did not consider the effects of size or placement of the loop within the outer boundary. Future work should consider additional factors, such as size, shape, count and location of inner loops, and investigate what features reveal about the complexity of the movement.

CHAPTER 3: METHOD FOR QUANTIFYING COMPLEX PHASE PLANE PORTRAITS

Abstract

Objective: The purpose of this study was to develop an automated method of approximating the area enclosed by complex phase portraits, validate the method's accuracy, and demonstrate its application with regard to computing a metric of motor performance, Phase Area Ratio (PAR). *Method*: Kinematic records of single joint motions were portrayed as phase plane portraits and assessed through an automated program. Three separate metrics were extracted from each phase portrait based on three locations within and around the phase portrait: (1) the inner loop, (2) the boundary, and (3) the convex hull. The areas enclosed by these designated groupings were computed by an approach based on computational geometry. Validity of the metrics was tested via performance measures. Additional assessments were done to compare the computation of PAR by the proposed area approximation method to that of an image-based method. A final assessment was done to understand how a state-space-based performance measure compared to other metrics of smoothness. *Results*: Designation of data points falling within a phase portrait via the automated program was completed with high-accuracy (*accuracy, sensitivity, specificity* > *96%*). Overall, the geometric area approximation and the alternative, image-based, area approximation algorithms correlated well ($\rho = 0.958$); however, there was not a strong correlation between these aforementioned methods and an alternative motor performance measure ($\rho = 0.235$). *Conclusions*: It is concluded that, the area approximation method for PAR developed herein, is highly accurate and

can have wide applicability to quantifying dynamic systems. Future work is recommended to better understand PAR's correlation to other measures of biomechanical performance, as well as any physical dynamic system.

Introduction

There is an existing need for reliable metrics of motor performance—one that is capable of capturing movement idiosyncrasies and demonstrates sensitivity. Previous groups have employed kinematic movement analysis as a means of identifying various features that differentiate ideal from impaired, and their efforts have led to a variety of performance metrics (Chang et al. 2008); however, the sensitivity of some features (i.e. number of movement units) is dependent on an arbitrary threshold for determining fluctuations in a velocity profile (Alt Murphy, Willen, and Sunnerhagen 2011). Measures offer improved sensitivity; one focuses on a feature referred to as 'residual excursion deviation' and represents the cumulative sum of deviation from the midsection of an angular position profile—a region that is expected to have constant velocity (Wininger, Kim, and Craelius 2009). Jerk, found by computing the third derivative of angular position, has been used by many but has also been criticized for yielding counterintuitive results (i.e., instances of non-monotonic metric response with increasingly complex motion) (Song, Tong, and Hu 2008, Rohrer et al. 2002, Cozens and Bhakta 2003, Goldvasser, McGibbon, and Krebs 2001). Previous work validated the effectiveness of phase portrait representation. Profiles of increasing anomaly, displayed and assessed in the phase plane, produced a phase metric that was less sensitive to size-based factors and avoided the bias that resulted from jerk-related metrics (Wininger, Kim, and Craelius 2012).

Phase portraits are a common means of graphically representing dynamic data. For biomechanical analysis, the phase domain is useful because it reveals the instantaneous relationship between force and velocity, without regard to timing. When the complexity of nonlinear differential equations interferes with interpretation, phase portraits provide a clear and simple tool for visualizing the system's dynamics and observe its qualitative behavior (Strogatz 1994).

Phase portraits have been used in a number of biomedical studies, including those involving gait analysis, heart rate patterns, eye movement and control, and joint kinematics, for the benefit of revealing behavior cyclicity (Beuter and Garfinkel 1985, DiBerardino et al. 2010, Eucker et al. 2001, Govindan et al. 2011, Polk et al. 2008, Riley et al. 1995, Serra et al. 2008, Wininger, Kim, and Craelius 2012). Hurmuzlu, et al.'s 1994 paper in the *Journal of Biomechanics*, discussing joint kinematics during human locomotion, recognized that temporal plots lacked the capacity to divulge details regarding the dynamic nature of joint kinematics and, therefore, turned to graphical techniques commonly used in nonlinear dynamics—phase portraits (Hurmuzlu, Basdogan, and Carollo 1994).

Beuter, et.al.'s work, focusing on the lower limb dynamics of children with cerebral palsy, noted that intersecting loops formed within a phase portrait may indicate a feature of motion complexity, since unimpaired control subjects generated smooth phase portraits, free of inner loops. The researchers theorized that the existence of intersecting loops was due to an additional variable, so rather than behaving as a second-order dynamical system, atypical motion involved an additional degree of freedom. Supported by the Fundamental Theorems of ordinary differential equations pertaining to existence-

uniqueness, Beuter, et. al. rationalized that a self-intersecting phase portrait was actually a two-degree projection of a higher-order system (Beuter and Garfinkel 1985).

Research groups have recognized the value of analyzing qualitative aspects of phase portraits and have sought ways to quantify complexity. DiBerardino, et al. used Elliptical Fourier Analysis (EFA), a method which accounted for irregularities in the elliptical shape, and measured complexity by the number of harmonics required to define a phase portrait's shape (DiBerardino et al. 2010). In 2011, Govindan, et al. used phase plane analysis to study fetal heart rate patterns (fHRP) by plotting the fetal heart rate (fHR) against its first derivative with respect to time and approximated the area enclosed within the trajectory, as a means of quantifying the nonlinear properties of fHR (Govindan et al. 2011). Additionally, phase portraits work well when describing single joint motion and provide insight into energy consumptions across the trajectory (Clark and Phillips 1993, Polk et al. 2008).

Phase plane analysis has the potential to be a powerful tool for diagnosis of motor disorders, as portraits accentuate aberrant, unsmooth movements, while graphically representing these idiosyncrasies as functions of position and velocity. In motor disorders like spasticity, where a high-velocity, passive movement triggers a position-specific "catch"—marking the start of an increased resistance to movement, phase portraits may capture the spastic event and provide a quantifiable record for diagnosis and treatment; this is a need that has yet to be met (Fleuren et al. 2010, Malhotra et al. 2009). The present study aims to develop a novel scheme for quantifying the area enclosed by complex phase portraits, validate its accuracy, and use the area-finding algorithm to compute a promising metric of motor performance.

Preceding Metrics & Algorithms

Phase Area Ratio (PAR) and Flood Fill Area Approximation

Our lab has focused on developing a measure of the deviation from an ideal phase portrait, which uses a process that quantifies areas within the portrait—hence termed the Phase Area Ratio (PAR). Three parameters are extracted from the phase portrait to compute PAR:

1. ***Footprint area (A_F)*** – the area enclosed by the phase portrait perimeter.
2. ***Hull Area (A_H)*** – the area designated by the smallest convex set, containing all data points.
3. ***Loop Area (A_L)*** – the area enclosed by inner loops, created as the trajectory wraps upon itself.

PAR is defined as:

$$PAR = 1 - \frac{A_F}{A_H + A_L} \tag{2}$$

In the case of a simple extension-flexion of a single joint, the ideal trajectory will yield a phase portrait that is smooth and elliptical. The ratio of actual trajectory to ideal trajectory signifies the efficiency associated with a reaching task. A PAR score of zero represents a highly efficient trajectory, free of inner loops or concavities; A PAR score will approach one as a trajectory becomes increasingly complex (Atler et al. 2015).

Recent work has focused on calculating the area within a phase portrait via a flood-fill imaging technique. The Flood-fill area approximation approach works by first converting generated phase portraits to binary images and, then, uses an iterative approach to approximate the areas within designated boundaries; each loop boundary constitutes a new layer, and the pixels within this boundary are used to approximate the

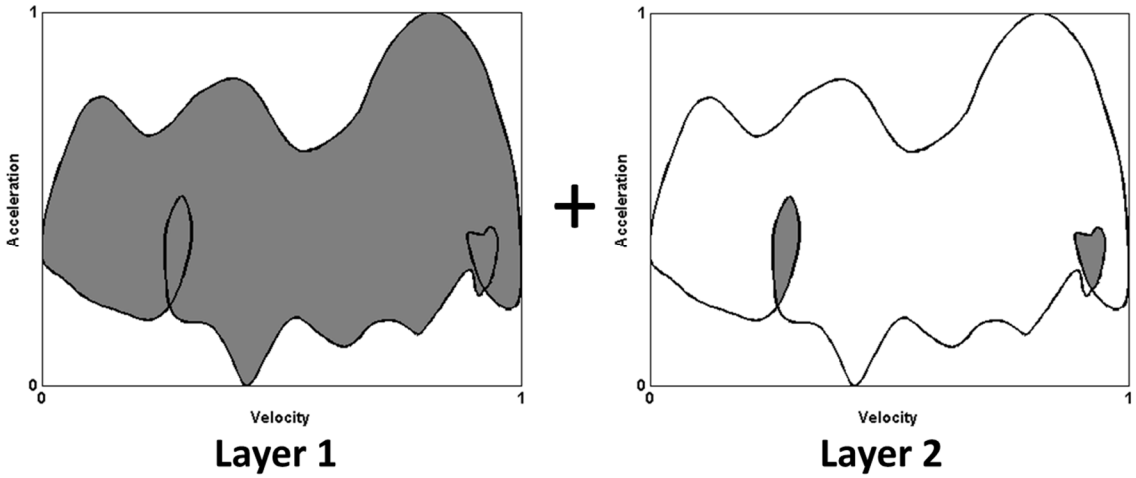

Figure 8: Layering technique incorporated in the Flood-fill approximation method

area (Figure 8). In the case where internal loops exist, as seen in complex movement patterns, each internal loop counts as a new layer, and the area (A_L) will be approximated, thus contributing to the overall PAR score (Atler et al. 2015).

Regional Excursion Deviation (RED)

Ideal motion produces a notably smooth trajectory, characterized by an accelerative onset, a period of constant velocity, followed by a deceleration to a desired endpoint. Non-smoothness is typified by transient accelerations-decelerations during the mid-region. Regional excursion deviation (RED) is a cumulative measure of the sudden accelerative bursts—or deviations from ideal velocity—that occur during single-joint motions, such as reaching, and is representative of non-smoothness. The scalar value of RED is defined as:

$$RED = \frac{1}{N}\int_{\Delta\theta} S(\theta)d\theta \quad (3)$$

where *S* is the spatial acceleration vector, which represents the accumulation of the errors, or deviation, from a trajectory path comprised of piecewise, linear segments (Wininger, Kim, and Craelius 2009). RED will be used as a comparative measure of smoothness, against PAR.

Methods

The current study supports the use of the PAR score, while introducing an alternative computational method to approximate the area bounded by a phase portrait, hereafter referred to as the Polyarea approximation method.

Polyarea Approximation Method

The Polyarea approximation method is based on the concept that periodic motion will produce a closed form when plotted in a phase space and uses computational geometry to quantify areas within the closed form. Ideally, the data points, representing the motion trajectory in space, yield a smooth, elliptical phase portrait. Connecting *n*-neighboring data points with *n*-line segments yields an n-sided polygon; thus, the greater the number of data points, the better the polygon approximates the true shape of the trajectory. The area within the n-sided polygon is easily computed using numerical analysis software built-in functionality. However, for complex trajectories, yielding two-dimensional phase portraits with self-intersecting loops or inner concavities, an n-sided polygon misrepresents the phase portrait and fails to properly assess the areas required by the PAR metric. To compute a PAR score, it is necessary to differentiate a boundary from an inner loop data point, as well as to determine which boundary points form the plot's convex hull and/or the plot's footprint. The next two sections, *Inner Loop Identification* and *Footprint and Convex Hull Data Point Identification*, describe the

development of an inner loop identification scheme and the designation of data points (inner loop, convex hull, and/or footprint) in the phase plot.

Inner Loop Identification Scheme

The method for detecting loops within phase portraits begins by searching for points of intersection in the curves. For this, an open source algorithm was appropriately adapted (Canós 2006). If intersection points are returned, the proposed points are used to test various criteria and eliminated, as needed. Due to scale differences, data are normalized and any points within a small radius (0.03 units) from the proposed intersection point are saved for inspection (Figure 9). A jump in indices within the radius suggests a possible loop formation; however, a jump in indices is only considered significant if it falls within lower and upper limits—the upper limit is needed to avoid having the outer boundary considered as a loop. Therefore, data points surrounding an intersection point result in the formation of an inner loop if the proposed loop is comprised of a minimum of 5 data points, while not exceeding a length of 60 percent of the entire data set.

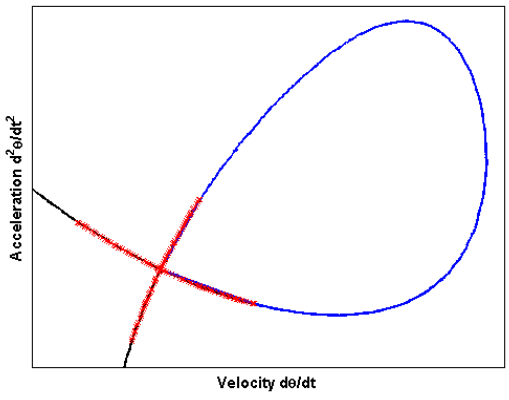

Figure 9: Demonstration of the inner loop identification scheme. Data points falling within a given radius from the intersection point are shown in red. A gap in the index values indicates the formation of an inner loop, as shown in blue.

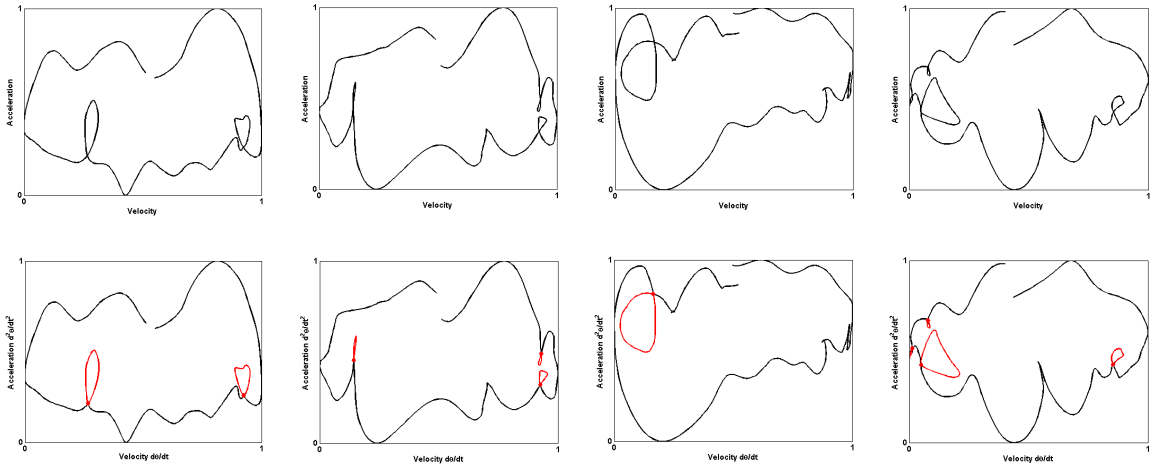

Figure 10: Inner loop identification within a series of complex acceleration-velocity phase portraits using the proposed algorithm

Loop Identification Performance Measure

Validation of the loop identification algorithm verifies that the algorithm accurately identifies all inner loops. This is done by visual inspection of processed phase portraits (Figure 10). The inspection is based on an "all-or-nothing" approach, classifying each phase portrait in its entirety rather than giving consideration to each inner loop. The phase portraits are categorized as follows:

1. ***True Positive (TP)***: The algorithm correctly identified all loops existing within a phase portrait.
2. ***True Negative (TN)***: The algorithm correctly identified no loops existing within a phase portrait.
3. ***False Positive (FP)***: The algorithm identified a minimum of one loop within the phase portrait that did not actually exist.
4. ***False Negative (FN)***: The algorithm failed to identify a minimum of one loop existing within a phase portrait.

The accuracy rate, sensitivity and specificity of the loop identification algorithm is expressed as:

$$Accuracy\ Rate = \frac{TP + TN}{TP + TN + FP + FN} \quad (4)$$

$$Sensitivity = \frac{TP}{TP + FN} \quad (5)$$

$$Specificity = \frac{TN}{TN + FP} \quad (6)$$

Footprint and Convex Hull Data Point Identification

A key element in the Polyarea method is to determine which data points form the phase portrait's convex hull and which points form the footprint. The convex hull is defined as the smallest subset of points that encapsulates the remaining points within the set (Graham 1972). The subset of points forming the convex hull is found using numerical analysis software built-in functionality, in which the complete data set (X,Y) serves as the input arguments and the function returns indices for the subset of convex hull data points (Figure 11).

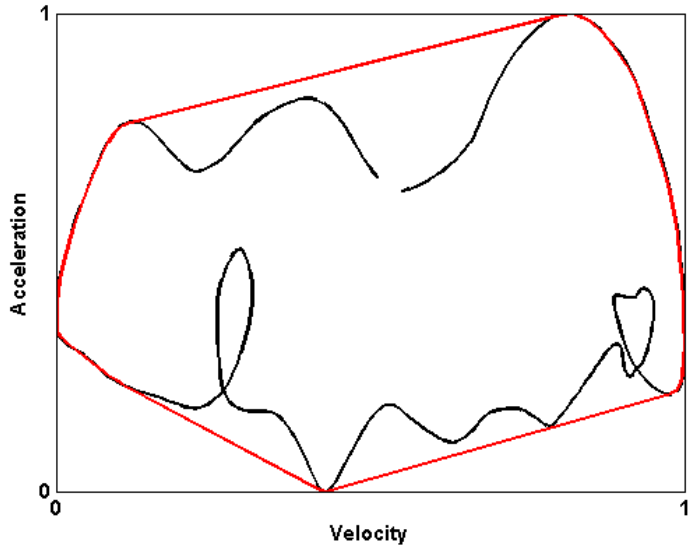

Figure 11: Convex hull of a complex acceleration-velocity phase portrait, shown in red

The method used to find the data points forming the phase portrait's footprint is based on alpha shape theory, developed and discussed in great depth in literature (Edelsbrunner, Kirkpatrick, and Seidel 1983, Edelsbrunner and Mücke 1994, Liang et al. 1998), but for the purposes of the present study, the most simplistic two-dimensional use was demonstrated. Edelsbrunner, et. al. related the alpha-shape to a "generalized convex hull", and for the cases where alpha approaches infinity, the alpha-shape represents the convex hull of a set of points. As alpha decreases to zero, the alpha-shape begins to wrap around bends until, eventually, it is small enough to follow along the true shape of the two (or, if desired, three) dimensional object, including existing inner concavities (Edelsbrunner, Kirkpatrick, and Seidel 1983). The proposed method uses an open source algorithm—modified for the purposes of this study—to compute the alpha shape (Lundgren 2010). The data points of the alpha shape (Figure 12) were then used to compute the area of the footprint, which—once again—was simply considered as an n-sided polygon.

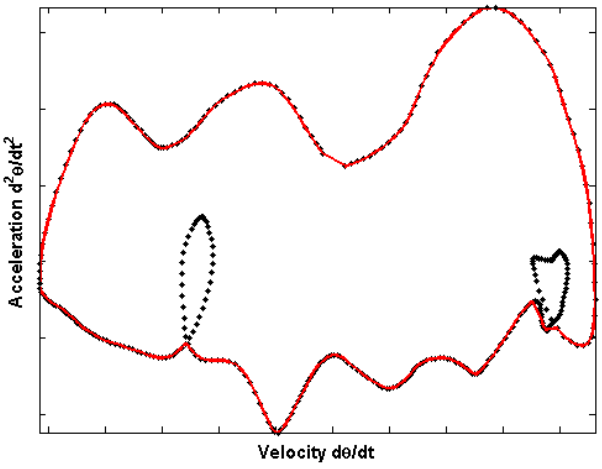

Figure 12: Footprint of a complex acceleration-velocity phase portrait, shown in red

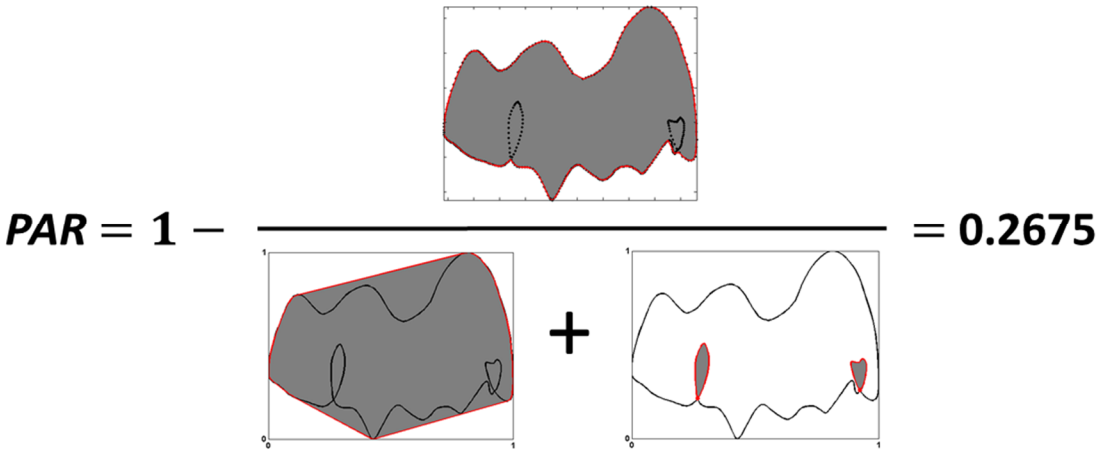

Figure 13: Representation of the PAR equation through two sets of phase portraits. (Top) Portraits are elliptical and resemble typical motion; (Bottom) Portraits show complexities, such as inner loops, suggesting atypical motion.

Results

A total of 1439 phase portraits of varying complexity were processed using the Polyarea method. Post-processing, the phase portraits were visually inspected to assess the accuracy of the inner loop identification algorithm, as summarized in Table 4. It should be noted that the visual inspection process was extremely conservative in its judgement and portraits were examined under high scrutiny. Regions where small loop formations were questionable were appropriately enlarged before judgements were finalized.

Table 4: Cases of Phase Portrait Inner Loop Identification

	True Positive	True Negative	False Positive	False Negative	Total
Identified Cases	430	968	24	17	1439

Results from the inspection revealed that approximately 67 percent of phase portraits did not have a loop formation within the convex hull, although inner concavities may or may not have been present, and these “true negative” cases were accurately identified by the algorithm. Likewise, for about 30 percent of the phase portraits designated as “true positive” cases, all loops within the convex hull were properly identified. Approximately 1.7 percent of the cases fell under the category of “false positive” and were identified as having at least one loop that did not actually exist. Only 1.2 percent of the cases were considered “false negative”, meaning that the algorithm failed to recognize at least one loop existing within the convex hull. Overall, the inner loop identification scheme performed with an accuracy rate of 97.2 percent, sensitivity of 96.2percent, and specificity of 97.6 percent (Equation 4 - 6).

Comparison of Polyarea and Flood-Fill Computation Methods

The areas of 1439 phase portraits were computed using both the Polyarea and Flood-fill methods. The phase portraits spanned a wide range of forms: from simple, elliptical forms to highly complex cases, comprised of inner concavities and intertwined looping patterns. Regression analysis was performed to study the relationship between the two methods. The scatter plot (Spearman rank correlation coef., $\rho = 0.958$; coef. of determination, $R^2 = 0.508$) depicted in Figure 14 (*left*) shows that—although there was a positive correlation between methods and a large portion of the area approximations followed a 1:1 ratio—the Polyarea method had more of a tendency to approximate higher PAR scores. A paired t-test revealed that the discrepancies in scores was significant ($t = 2.25$, $p = 0.0245$); however, it should also be noted that the 95 percent confidence interval was from 0.00055 to 0.0080, so the mean difference in pairs was significant but small.

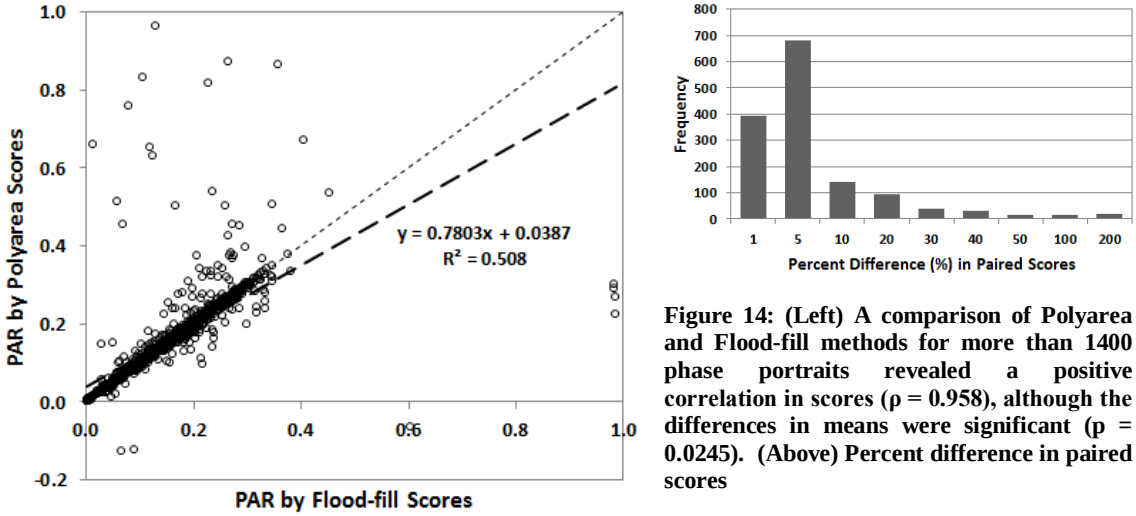

Figure 14: (Left) A comparison of Polyarea and Flood-fill methods for more than 1400 phase portraits revealed a positive correlation in scores (ρ = 0.958), although the differences in means were significant (p = 0.0245). (Above) Percent difference in paired scores

Additionally, 75 percent of the paired scores had a percent difference of less than 5 percent (Figure 14(*above*)).

Cases of Discrepancy: Polyarea vs Flood-fill Approximations

Discrepancies between Polyarea and Flood-fill approximation methods were investigated further and focus was directed toward the phase portraits that deviated far from the identity line ($PAR_{Polyarea} = PAR_{Flood\text{-}fill}$). There were three main causes for discrepancies; the first two scenarios resulted in unreasonably high PAR by Polyarea scores, while with the third scenario, results reversed and PAR by Flood-fill approximation scores were erroneously high (Table 5).

In cases where PAR by Polyarea scores were excessively high, close examination of the phase portraits found that these portraits shared a similar feature—a sufficiently large gap between the first and last data point, as illustrated in Figure 15 (a). Interestingly, this gap only affected PAR by Polyarea scores when the first and last data points had unequal velocity values; cases where the first and last data point had equal

Table 5: Scenarios for Large Polyarea-Flood-fill Approximation Discrepancies

Scenario	Description	Result
1	Large gap between first and last data point. Data points have unequal velocity	High PAR by Polyarea scores
2	Sparse data points affected alpha-shape footprint area approximation	High PAR by Polyarea scores
3	Cusped or pinched portrait	High PAR by Flood-fill scores

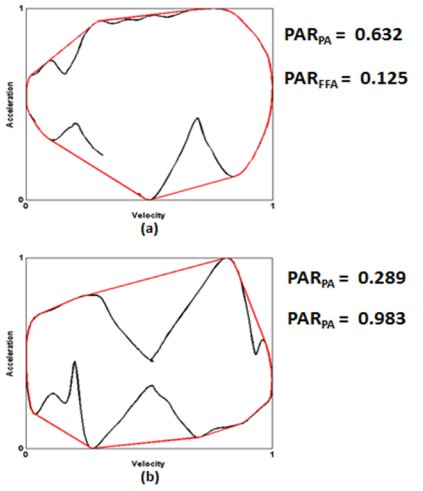

Figure 15: Phase portraits for (a) Case 1 and (b) Case 3, in which large discrepancies exist between Polyarea and Flood-fill approximation methods

velocity values (i.e. one point was directly above or below the other) did not yield noticeable scoring differences between the two approximation methods. This feature affected the calculation of the footprint area, resulting in inaccurately low approximations; however, it is unknown why portraits were unaffected in cases where the first/last point had equal velocity.

A second scenario for excessively high PAR by Polyarea approximation scores also occurred during calculation of the footprint area. Further assessment showed that fine-tuning the alpha value in the alpha-shape algorithm improved the outcome and resulted in a PAR by Polyarea value that nearly matched the PAR by Flood-fill approximation value. Since the issue was resolved through alpha-value adjustments, it is believed that the second scenario resulted when the data points forming the outline of the footprint were sparse. In essence, the second scenario may be thought of as an alpha-shape with too small of radius, circulating around the shapes perimeter, slipping past the

gap between two data points, and becoming trapped within the phase portrait; thus, the footprint area is approximated to near-zero.

The third scenario reversed the outcome with unreasonably high PAR by Flood-fill scores. Figure 15 (b) shows the common shape for this scenario: a phase portrait free of inner loops but with a pinched—or tipped hourglass-type—perimeter. It is unknown why the flood-fill, image-based algorithm is sensitive to this specific shape. However, one should note that although a large discrepancy between scores was prevalent for this specific footprint shape, there were a few instances where the Flood-fill and Polyarea approximation methods were compatible.

Assessment through Modelling

To better understand small discrepancies between the area approximation methods, phase portraits were modeled as simple circles, where one large circle enclosed one to many circles of smaller radii. Each circle shared the same center point, so the Polyarea method's loop identification was not utilized during this basic comparison, though its accuracy was previously confirmed. Testing under the Flood-fill method, validated both the method's ability to identify loops and approximate loop area.

Ten test cases, with inner looping patterns, were modeled and provided insight into looping scenarios, ranging from low to high complexity. For this model, the term *complexity* described the internal looping pattern, where *low complexity* was the case of one to few internal loops, having large to mid-size radii, and *high complexity* was the case of several internal loops, ranging in sizes from large to small.

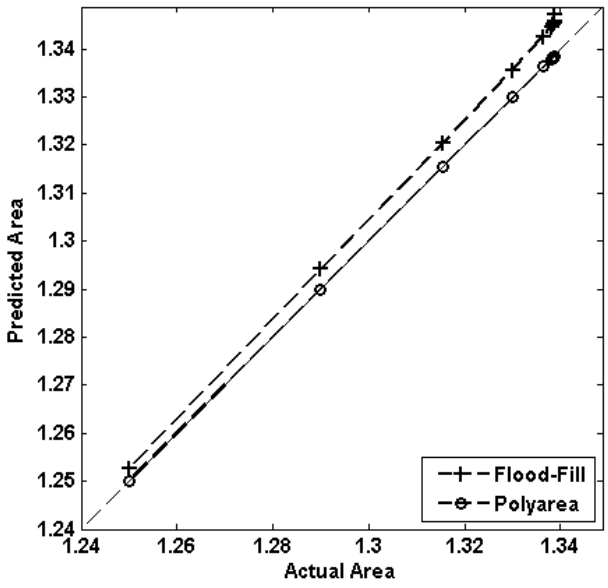

Figure 16: Comparison of predicted area (Flood Fill vs Polyarea) and actual area

Results from this basic circular-patterned model indicated that the Polyarea method provided an accurate area approximation. It is important to note that the accuracy of the Polyarea method is dependent on the number of data points (i.e. fewer data points leads to a less accurate approximation), so in data collection, particular care must be given to the sampling rate.

The accuracy of the Flood-fill method is related to image resolution and proper identification of a loop. There are a few drawbacks that exist when using the Flood-fill method. As shown in Figure 16, one drawback is that the method has a tendency to slightly overestimate area. Also, the Flood-fill method requires greater computation time, as it locates loops and estimates area "layer-by-layer". Third, while testing high complexity levels in the circle model, the Flood-fill method had difficulty locating circles that were small (radii < 0.01) and with approximately equal radii.

Comparison of PAR and RED Computation Methods

The kinematic data from the extension-flexions, which had been used to generate the 1439 phase portraits analyzed by PAR, were divided into at the transition from extension to flexion; RED scores were computed for each, and then averaged. The averaged RED scored was then paired with its PAR counterpart and analysis followed. Regression analysis was performed to study the relationship between the PAR and RED methods. The scatter plot (Spearman rank correlation coef., $\rho = 0.235$) depicted in Figure 17 shows that the correlation between PAR and RED scores was negligible. The spread of scores shows that the majority of PAR scores held between 0 and 0.3 units, while RED scores spanned between 0.2 to 0.8 units.

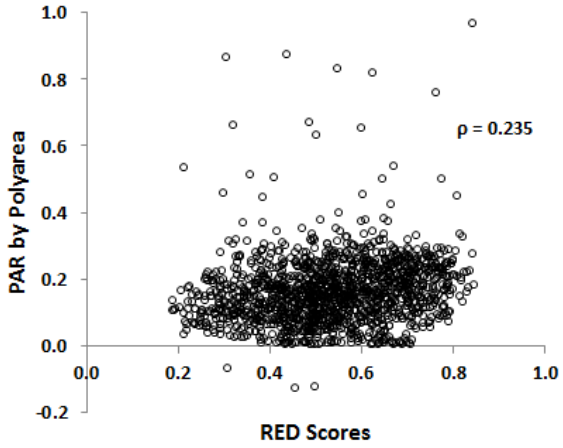

Figure 17: Comparison of PAR scores by Polyarea approximation method with RED scores.

Discussion

Demonstrated by the present study, Phase Area Ratio (PAR) is a viable metric to quantify dynamical system but depends on a robust area approximation scheme, well-equipped for complex phase portrait. Herein, the development of the Polyarea approximation method was highlighted—an automated method that distinguishes whether

a data point belongs to an inner loop, the outer boundary points, or possibly both, and then approximates the areas within these designated groups. The loop identification scheme was shown to have high performance ratings (*Accuracy*, *Sensitivity*, *Specificity* > 96 %).

Additionally, the two computational methods—Polyarea and Flood-fill—approximated the area bound by a phase portrait with similar results ($\rho = 0.958$). PAR scores computed based on Polyarea approximation have a tendency to be slightly higher than those based on Flood-fill approximation, which is reasonable since flood-filling over-estimates areas in basic models. Cases of rare, extreme discrepancies in scores exist at the fault of both methods, indicating nuances in phase profiles affect each method to varying degrees.

When PAR scores were compared to RED, a negligible correlation was found between performance measures. RED scores spanned over a region of 0.6 units; PAR scores were mostly within a 0.3 unit region, with a portion of the drifting points attributed to aforementioned erroneous measurements. Based on the assessed trajectories, it is apparent that RED is more sensitive to nuances in trajectories, especially since the scores presented in Figure 17 were computed as averages—thus, diminishing the maximum and elevating the minimum. Although highly respected, it should be noted that RED, nor any metric—for that matter, is not a "gold standard" score. It is suggested that future work focuses on a model-based confirmation of these results.

There is currently no well-accepted, standard measure of movement efficiency, and an ongoing effort to understand how the central nervous system (CNS) processes key information in one's environment and chooses to direct the musculoskeletal system to act

to accomplish goal-oriented tasks. Previous groups hypothesized that the CNS acts to minimize energy expenditures, although it was found not to be the case in models and in subjects with no known neurological or musculoskeletal disorders (Alexander 1997, Kistemaker, Wong, and Gribble 2010). Hemiparetic subjects, however, have shown a significant increase in energy expenditures over control counterparts to complete activities of daily living, such as dressing and walking (Singh et al., 2011, Detrembleur et al. 2003). Therefore, although energy costs may not be a primary concern of the CNS, a decrease in energy expenditures to complete a given task may serve as an indication of improved function and an effective treatment protocol.

The area enclosed by an acceleration-velocity phase portraits equates to specific power (power per unit mass). Typical motion generates phase portraits that are smooth, elliptical and near symmetrical. In complex cases—portraits with asymmetrical irregularities, including inner looping and concavities—that deviate from the expected shape, it is hypothesized that power dissipated during these movements is directly proportional to PAR scores. It is, therefore, recommended that phase portraits may be used in future work to study efficiency of impaired movement.

Conclusions

Representation of the data in phase profiles provides a highly valuable and progressive tool for viewing and quantifying impaired motion. Herein, the Polyarea approximation method was presented, validated and its use demonstrated in a metric of motor performance, PAR. The Polyarea method incorporates a high-accuracy scheme for differentiating points within a phase plane and, except for unusual cases, also computes the areas bounded by data points with high accuracy, while requiring negligible

computational time. It is recommended that the Polyarea area approximation method be pursued in future studies to quantify motor performance via the PAR metric.

PAR shows promise as a clinically relevant measure of motor performance, as it provides a comparison of the true area to the optimal area designated by a kinematic trajectory represented in phase space. It was shown that PAR may not be as sensitive of as measure as RED. However, the benefits of the PAR metric are three-fold: 1. it is scale-independent, 2. it is based only one assumption: optimally efficient motion transcribes a symmetrical phase portrait that is free of inner loops and concavities, and 3. it is bounded by 0 and 1, respectively classified as *Perfectly Efficient Motion* and *Completely Impaired*. Thus, PAR is an applicable assessment of discrete movement and may be used to assess a wide range of impairments. Future work is recommended in two areas: 1. To pursue a model-based approach to establish PAR's sensitivity to profiles of increasing anomalies, and 2. To establish correlations between PAR and clinical scales.

CHAPTER 4: QUANTITATIVE ASSESSMENT OF SPASTICITY BY PHASE PLANE ANALYSIS

Abstract

Objective: The objective of this study was to demonstrate the use of the Phase Area Ratio (PAR) metric to track progression of SPMS subjects, receiving anti-spasticity drug treatment. Additionally, this study aimed to show that PAR is a useful tool to improve inter- and intra-rater reliability, draw comparisons within and across subjects, and provide a means to study factors affecting movement, including pace-dependencies and limb differences. *Method*: MS patients (N = 12; 47.8 ± 9.9 years, 8M/4F), with no recent history of treatment with anti-spasticity agents, and matched controls (N = 8; 49.5 ± 13.2 years, 5M/3F) were tested at baseline and after a one-month period, during which the MS patients were administered a dosage of oral baclofen. Clinical assessments included the Modified Ashworth Scale (MAS) and Tardieu Scale (TS). Kinematic performance was measured as subjects performed single-joint extension-flexions at the elbow using the Mechanical Arm and Support Tracker (MAST). Testing was completed on both arms and at three defined paces, against a resistive torque. Processed kinematic data were displayed in a phase plane portrait and quantified using PAR. *Results*: Traditional clinical measures indicated that, overall, participants did not show a significant improvement during the treatment period (MAS: $p = 0.050$; TS V1: $p = 0.36$; TS V2: $p = 0.025$; TS V3: $p = 0.21$). Although there were some individual improvements, the testing session was not a significant factor in PAR scores (*Slow*: $p = 0.48$ *Moderate*: $p = 0.80$; *Fast*: $p = 0.90$). Across subjects, PAR scores were significantly

dependent on the movement pace ($p < 0.0001$). It was also revealed that there were not significant differences between limbs ($p = 0.33$). Conclusions: It is concluded that the PAR metric provided an objective means of tracking patient progression, while promoting inter- and intra- rater reliability. Additionally, the metric allowed for comparisons to be drawn within and across subjects, as well as revealed influential factors affecting movement.

Introduction

Spasticity and Assessment

A major symptom of multiple sclerosis (MS) is spasticity, reportedly affecting up to 90 percent of patients (Burridge et al. 2005, Physicians 2009, de Sa et al. 2011). The most widely accepted and commonly used measures of spasticity are the Ashworth and Modified Ashworth scale (MAS), which are a subjective assessment of the resistance to stretch when an affected limb is passively moved (Bohannon and Smith 1987). Despite its routine use, the MAS lacks quantitative support, has poor inter-rater reliability and the inability to distinguish neurogenic components of spasticity from mechanical (Bandi and Ward 2010, Haas and Crow 1995), leading various groups to promote alternative assessments (Alibiglou et al. 2008, Fleuren et al. 2010). A similar metric, the Tardieu Scale (TS), is also evaluated during passive limb movement—over slow, fast, and with gravity test variations—and notes whether a spastic event, or “catch”, is or is not triggered at a precise angle (Bandi and Ward 2010). Criticism of Tardieu’s subjective nature and poor reliability also applies to MAS (Ansari et al. 2008).

Treatment

Spasticity management comes in a variety of forms, including physical, occupational, and robotic therapy (Bandi and Ward 2010, Beard, Hunn, and Wight 2003, Physicians 2009, Hefter et al. 2012, Rohrer et al. 2002, Solari et al. 1999). Pharmacological treatments have shown to improve, temporarily and by varying degrees, a patient's ability to manage typical activities of daily living (ADL) and regain some independence (de Sa et al. 2011). Anti-spastic agents, such as baclofen, have been effective in reducing spasms and ameliorating pain associated with spasticity (Sawa and Paty 1979, Scheinberg et al. 2006). High-dosages of oral baclofen are often required to achieve clinical effectiveness but relief is accompanied by a high incidence of side-effects, including dizziness, drowsiness and seizures (Scheinberg et al. 2006). Thus, a non-subjective, inter-rater reliable metric is needed to quickly assess the effectiveness of interventions, allowing a treatment team to closely monitor patient progression and adjust accordingly.

The present study aims to quantify motor performance of a sample of MS subjects, undergoing treatment with the anti-spasticity agent baclofen, and control subjects via the objective, Phase Area Ratio (PAR) metric. It is hypothesized that 1) the objective PAR metric will provide a means of tracking a subject's progression through treatment (intra-subject), as well as the ability to draw general comparisons across the subject pool (inter-subject), and 2) the PAR metric may not correlate well with established clinical measures but may correlate with treatment.

Methods

Subject Pool

Twelve subjects suffering from Secondary Progressive Multiple Sclerosis (SPMS) and receiving treatment at the VA Medical Center in Washington, D.C. and eight matched control subjects participated in this study; demographic information is presented in Table 6. Participants in this study met the following criteria: 1) minimum of 20/40 visual acuity in at least one eye, 2) older than 18 years, and 3) no known cognitive impairments, preventing compliance with the research protocol or the ability to provide informed consent. Approval for subject testing was granted by Rutgers IRB, and all participants gave informed consent. Additionally, the subjects within the MS cohort fulfilled the following requirements: 1) classified as SPMS a minimum of 12 months prior to the study, 2) diagnosed with spasticity in an arm and a leg, and 3) had no prior history of other neurological disorders (e.g. stroke, epilepsy) or severe psychiatric disturbance (e.g. schizophrenia, psychosis).

Limb spasticity among the MS subjects ranged from mild to moderate in degree; treatment for these limbs with standard anti-spasticity medications had either been under-dosed or never prescribed. Upon entering the study, participants receiving pharmacological treatment ceased medication and allowed system clearance for 30 days before the study commenced.

Table 6: Participant Demographics

Descriptor	**MS Patients (N=12)**	**Control (N=8)**
Age: mean ± std (min, max)	47.8 ± 9.8 (30, 63)	49.5 ± 13.2 (28, 60)
Sex: M/F	8/4	5/3

Study Design

Assessment of a limb spasticity occurred at two distinct sessions, separated by a one month gap, within the study. Clinical assessments (MAS and TS) were administered by both a neurologist and a physical therapist, and an average of these two served as the final clinical measure. After the baseline testing session (Session 1), participants were prescribed baclofen (30-90mg, Q8h, as recommended by published guidelines (Beard, Hunn, and Wight 2003) and titrated until the optimal dose (i.e. therapeutic benefit without side effects) was reached for each individual. Biomechanical assessments were also administered prior to treatment and one-month post-treatment.

Instrumentation and Test Protocol

Participates were securely positioned—with arm supported along a horizontal plane, free from gravitational influences, and elbow aligned with a goniometer—in the Mechanical Arm and Support Tracker (MAST) (Wininger, Kim, and Craelius 2009). Data were gathered from a potentiometric goniometer and accelerometer (ADXL330) by a LabVIEW (NI Instruments) graphical user interface (GUI), and goniometric data (i.e. angular position) was routed to a real-time biofeedback display. A resistive torque of 9 N-m was applied constantly throughout the extension-flexion repetition (Pousson, Lepers, and Van Hoecke 2001).

The HARI microcontroller unit (HMU, Nian-Crae, Inc.) collected data from the MAST sensors. The HMU, containing a Silicon Laboratories C8051F340 processor, utilized four of twelve channels for data collection at a sampling rate of 200 Hz. A computer interface allowed the therapist to calibrate the MAST and select the recording

mode, displayed a movement pacer bar for subjects to track during each trial, and recorded incoming data.

During testing, a therapist instructed subject to perform single-joint extension-flexions of the elbow according to protocol. Testing was completed using both the right and left arms at three defined paces, guided by a pacing bar displayed on an external monitor; the three paces (slow, moderate, and fast) corresponded to approximate angular velocities of 133 degrees/s, 200 degrees/s, and 400 degrees/s, respectively. The duration of each trial was approximately 60 to 90 seconds; the average number of repetitions for each trial was 6.2 ± 1.3 for slow, 6.7 ± 1.4 moderate and 7.3 ± 2.0 fast paces.

Signal Processing

Kinematic data gathered from twenty subjects was used to generate acceleration-velocity phase portraits. Prior to generating the portraits, data collected from the goniometer and accelerometer was filtered using a 2-way, 1^{st}-order butterworth filter with 5 Hz cutoff. Velocity data was computed by numerical differentiation of the position data gathered by the goniometer. Repetitions—designated as a complete flexion-extension cycle— were separated via an automated Matlab (The Mathworks, Inc.) program, using angular threshold filtering. Threshold values were adjusted, accordingly, after visually inspecting each subject's sequence of repetitions. To adjust for amplitude differences, the data-series were normalized to a scale of 0 to 1.

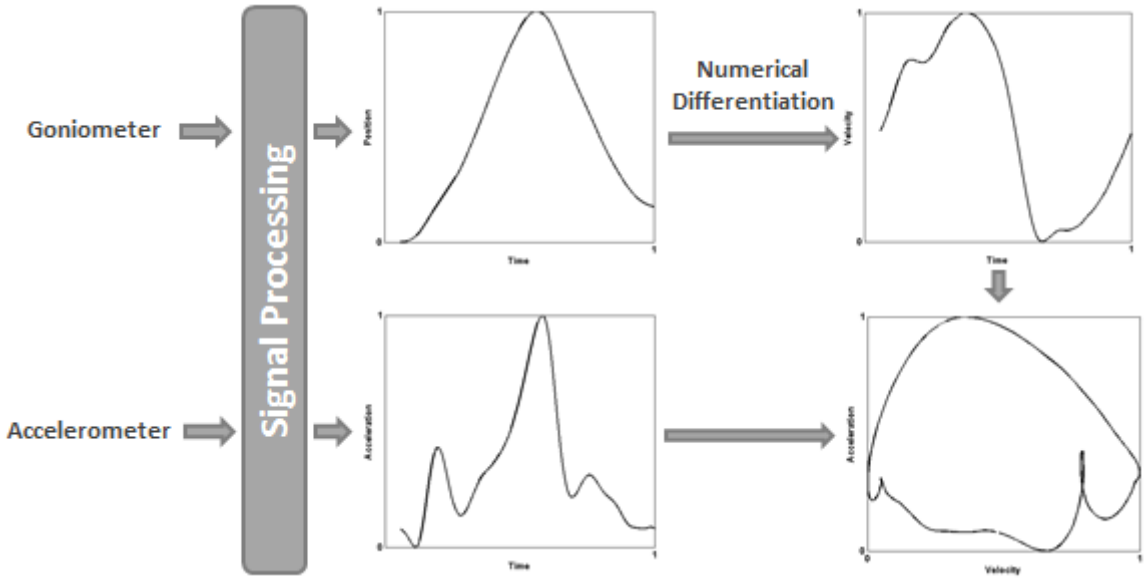

Figure 18: Overview of data collection to phase portrait process: data was collected through a goniometer and accelerometer, velocity was computed by method of central differences, and in the final step, A-V phase portraits were constructed in preparation for PAR metric assessment.

Performance Measure

PAR scores were computed using acceleration-velocity phase portraits, with the area assessed by the Polyarea Approximation (PA) methods. PAR is defined as:

$$PAR = 1 - \frac{A_F}{A_H + A_L} \tag{7}$$

where A_F is the footprint area, A_H is the hull area, and A_L is the total inner loop area. PAR scores were computed for each repetition of each unique trial (session-, pace-, side-specific).

Statistical Analysis: Development of a linear regression model

A mixed effect linear regression model was developed and the significance of each factor on the response variable, PAR scores, was analyzed using R (Team 2013). The models considered combinations of fixed and random factors, in which three factors (*Session*, *Pace* and *Side*)—with pre-determined, set levels that were fully tested across

subjects—were designated as fixed effects, and one factor (*Subject*) was treated as a random effect due to the fact that the subject pool was a sample of greater population. *Session*, initially modeled as a nested term within *Subject*, was designated as fixed effect to satisfy Bates's six-level-minimum guidelines (Bates et al. 2014, Bates D 2015). Therefore, the models were developed using only subjects that participated in a minimum of two test sessions (1240 repetitions in total). Through the random effect term, the proposed regression model accounts for a lack of independence due to multiple responses from each subject, as well as similar responses from multiple subjects.

The model was adapted, tested, and compared, as suggested in previous studies, using the R *nlme* package to perform hypothesis testing on a constrained (null) model and a full (alternative) model (Mehtätalo 2013, Pinheiro and Bates 2000, Pinheiro J 2015). The F-test, based on restricted maximum likelihood (REML), was used to compare models with modified fixed terms, and the Likelihood-Ratio-Test, based on maximum likelihood (ML), was used to compare random intercepts and slopes between models (Pinheiro and Bates 2000).

Additionally, models were assessed according to the assumptions of linear regression: linearity and lack of collinearity, homoscedasticity, normality of residuals, absence of significant outliers, and independence. As previously stated, incorporation of the random effect terms was thoughtfully done to account for lack of independence among responses. Assessment of preliminary models through a histogram of residuals and quantile-quantile (*q*-*q*) plots showed the data followed a normal distribution, although there was slight, unidirectional tailing. Data that strayed from the trend line were not considered outlying points, due to the expected variation in performance from

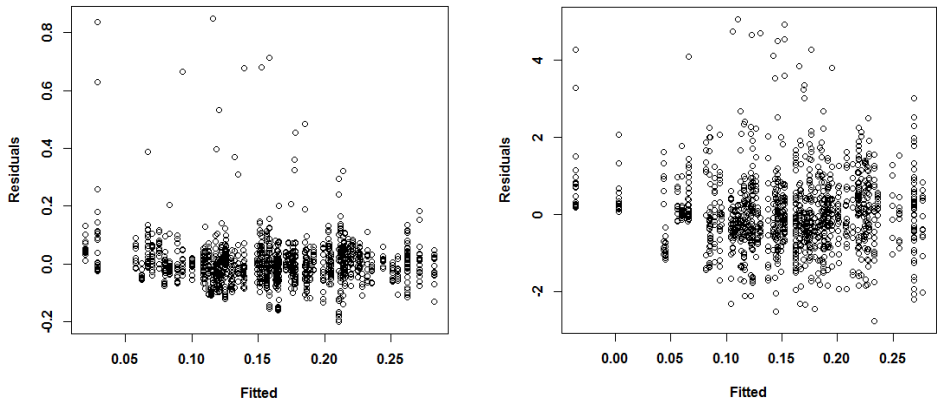

Figure 19: Residual plots pre- and post- inclusion of a weighted variance function.

impaired subjects. The plot of the residuals verses fitted values was checked for heteroscedasticity, and the Bartlett's test for the homogeneity of variances revealed unequal variances for *Subject*, *Session* and *Pace* ($p < 0.0001$ for *Subject*, *Session* and *Speed*; $p = 0.014$ for *Side*) (Bartlett 1937). It is warned that heteroscedasticity may interfere with interpretation (Zuur 2009). Data transformation is considered ill-advised by some, so for succeeding models, a weighted variance function that accounted for residual variance differences across subjects and movement speed was incorporated into the modeling scheme (Mehtätalo 2013).

Results

Unforeseen at the time of testing, hardware issues disrupted the accelerometer sensors signal, resulting in data with a too high of a signal to noise (SNR) to be recovered for five subjects. Analysis was completed using data from the remaining fifteen participants.

Clinical Measures

Clinical assessments were performed by the treatment team using the MAS and TS prior to treatment and after completing one-month of baclofen treatment. The MAS

scores, presented in Table 7, were based on individual scores assigned to the wrist flexor, wrist extensor, biceps, and triceps for both the left and right arm. Similarly, TS scores were calculated using scores from the wrist and elbow for both arms. Due to the non-normality in scores, the median values from Session 1 and Session 2 were compared using the Wilcoxon Rank Sum test. The Wilcoxon Rank Sum test also handles repeated measures, as is the case with each subject having a score for their left and right arm. Originally blinded to subject labels, a comparison of the entire subject pool (MS and control) distributions of Session 1 and Session 2 clinical measures showed that overall there was not a significant difference between sessions (MAS: V = 824.5, p = ; TS V1: V = 69, p = ; TS V2: V = 190, p = 0.029; TS V3: V = 240, p = 0.080).

Table 7: Clinical Measures

Measure	Session 1	Session 2	p-value
MAS	0.65 ± 0.87	0.47 ± 0.66	0.061
TS*			
V1	0.32 ± 0.60	0.27 ± 0.58	0.59
V2	0.60 ± 0.87	0.35 ± 0.63	0.029
V3	0.87 ± 1.03	0.65 ± 0.78	0.080

NOTE – Measures reported as mean ± std
*V1 – slow movement; V2 – under effects of gravity; V3 – fast movement

Phase Portraits and Kinematic Data Measures

Visual inspection of phase portraits provided insight into the complexity of the dynamical system. Figure 20 is an example of the acceleration-velocity phase plane portraits generated by a subject. The phase portraits show a noticeable reduction in complexity, i.e. inner looping and concavities, as the movement pace increases from slow to fast.

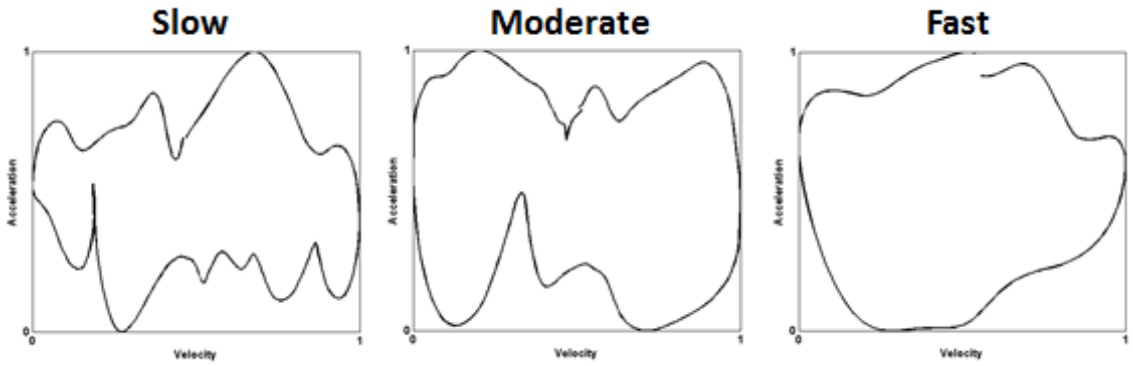

Figure 20: AV phase plane portraits generated while moving at slow, moderate, and fast paces. The portraits become increasing smooth and more elliptical as the movement pace quickens. As depicted in the lattice plots (Figure 22), this was a similar trend across subjects, session and side tested.

Boxplots were initially used to assess the effects of each factor on PAR values. Figure 21 (*Top*) compares subject performance at moderate pace during Session 1 (*Baseline*) testing. A scan of boxplots of PAR scores by subject shows the variability among subjects. The median PAR score fluctuated greatly across subjects from about 0.0120 to 0.222 during Session 1 and 0.107 to 0.246 during Session 2, with some subjects showing a larger spread in scores than others. Interestingly, it was expected that the subjects generating a greater median score would also have a higher variance among scores, but this hypothesis is unsupported by this initial assessment. When assessing the moderately paced repetitions, visually, there is not a consistent improvement (reduced median score or deceased variance) across subjects. The variance improved from Session 1 to Session 2 for subjects S56, S74 and S86 while the median score remained nearly the same; alternatively, the median score noticeably dropped for subject S89, while the variance changed little. For the few subjects, such as S10 and S89, that improved in both median score and variance, it is questionable whether the improvements were significant. The median line also indicates slightly skewed data among several subjects. The change

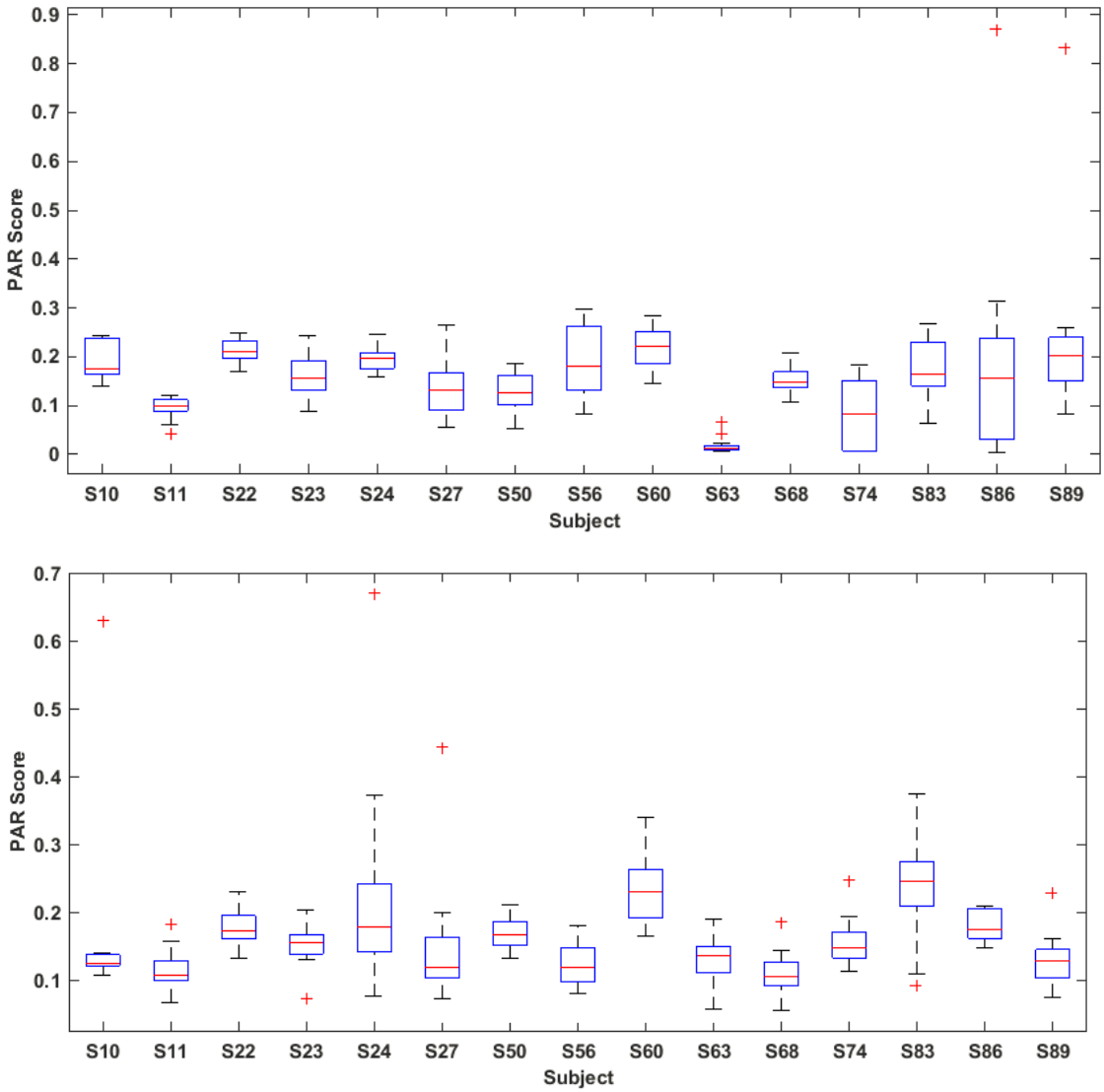

Figure 21: Inter-subject comparison of PAR scores assessed during baseline Session 1 (*Top*) and Session 2(*Bottom*). All repetitions were performed at a moderate pace.

in average PAR scores was an increase of 12 percent ± 92 percent (SE) from Session 1 to Session 2. Likewise, the change in average PAR scores generated at slow and fast movement paces was an increase of 18 percent ± 67 percent and decrease of 6.5 percent ± 120 percent, respectively, from Session 1 to Session 2.

Lattice plots were created via R's *lattice* package to display the range of PAR scores generated by each subject based on the testing factors (*Session*, *Pace*, and *Side*),

Figure 22: Lattice plots showing the effect of testing pace (fast, moderate, or slow) on PAR scores, broken down by subject, session (1 or 2), and side (left or right). Each point represents an extension-flexion repetition.

allowing for comparisons both between and within subjects, shown in Figure 22 (Sarkar 2008). The lattice plot indicated that most subjects performed similarly on both arms, and the majority of subjects did not have a visible difference across sessions. Nearly all subjects showed that PAR scores increased with decreased movement pace, leading one to believe that this trend is not condition-specific (healthy vs impaired). However, a few subjects (S63, S74, and S86) produced more homogeneous scores across the various paces during the first testing session and established the indirect relationship between

PAR scores and movement pace during the second testing session, provoking the question whether this could be a feature of typical or atypical behavior rather than just circumstance. Subject S86 showed a possible drop in average score and improved variance from Session 1 to Session 2 on the left side, whereas it appears that the average score increased slightly for subject S83 across sessions. Insight gained by the lattice plots, such as how the variability across subjects influenced the heteroscedasticity of the data, provided a foundation for preliminary regression models, and the development of these models is further discussed in the next section.

Overview of Mixed-Effect Models

Mixed-effect linear regression models were developed to further study the influence of certain factors on PAR scores. While blind to the subject labels (MS or control), initial models were based on all subjects. As stated previously, the model incorporated the random effect *Subject* and considered three factors—*Session*, *Pace*, and *Side*—as fixed effects, testing each individually and for interactions.

Testing revealed that the movement pace was a significant factor in the model ($F(1,1221) = 245.7$, $p < 0.0001$), and when tested in combination with the other factors, *Pace* remained significant (all scenarios, $p < 0.0001$). When considered alone, the testing session (baseline vs. follow up) was not a significant term in the model ($F(1,1222) = 2.66$, $p = 0.103$), and as the other factors were incorporated into the model, with *Session* as the first fixed effect listed, the influence of testing session remained non-significant under all circumstances (*Session* + *Pace*: $F(1,1220) = 3.39$, $p = 0.0659$; *Session* + *Side*: $F(1,1221) = 2.94$, $p = 0.0867$; *Session* + *Side* + *Pace*: $F(1,1219) = 3.79$, $p = 0.0517$). Unexpectedly, when Session was tested in combination with Pace and Side, with Pace as

Table 8: Summary of Fixed Effect Significance (All Subjects)

Fixed Effect	**Num DF**	**Den DF**	**F-value***	**p-value**
Date	1	1222	2.66	0.103
Pace	2	1221	245.7	< 0.0001
Side	1	1222	0.965	0.326
Pace*Session	2	1218	4.35	0.0131
Pace*Side	2	1218	2.64	0.0715
Session*Side	1	1220	0.661	0.417

*F-test based on REML

the leading factor, the testing session became arguably significant ($F(1,1219) = 4.18$, $p = 0.0411$), and this bordered as significant. It was believed that this was due to an interaction effect between *Session* and *Pace* but may also be a result of an approximation error introduced by the REML method. Throughout testing, the side (left or right) used during testing was not significant (*Side*: $F(1,1222) = 0.965$, $p = 0.326$; *Side* + *Pace*: $F(2,1220) = 1.23$, $p = 0.269$; *Side* + *Session*: $(1,1221) = 1.22$, $p = 0.270$; *Side* + *Speed* + *Session*: $F(1,1219) = 1.66$, $p = 0.198$). Additionally, there was a significant interaction between *Pace* and *Session* (*Pace-Session*: $F(2,1218) = 4.35$, $p = 0.0131$); however, interactions between the remaining terms were not significant (*Pace-Side*: $F(2,1218) = 2.64$, $p = 0.0715$; *Session-Side*: $F(1,1220) = 0.661$, $p = 0.417$). Table 8 summarizes the fixed effect findings.

Additionally, the model was modified to consider the individuality of each subject. Subject-specific slopes for the three fixed effects—*Session*, *Pace*, and *Side*, tested independently and with modified model terms, each had a significant effect (*Session:* LR= 129.6, $p < 0.0001$; *Pace*: LR = 27.9, $p < 0.0001$; *Side*: LR = 11.3, $p = 0.0035$).

Table 9: Summary of Subject-specific Random-slope Models (All Subjects)

Random Slope	**LR**	**p-value**
Session	129.6	< 0.0001
Pace	27.9	< 0.0001
Side	11.3	0.0035

*LR based on ML

Assessment of Parameter Estimates

The intercept of the models provided the mean PAR score for the baseline scenario. Depending on the factors tested, the baseline described subjects tested using their left arm, at a fast pace, and during Session 1.

As reported in Table 8, the pace of motion was the only fixed effect that had a significant effect on PAR scores. The intercept, or average PAR at a fast test pace, for this model was 0.111 ± 0.0108 (SE) ($p < 0.0001$). PAR scores increased by 40 percent (0.0448 PAR units, $p < 0.0001$) as subjects switched from a fast to moderate pace, and scores increased by more than 85 percent (0.0960 PAR units, $p < 0.0001$) when subjects switched to a slow pace.

With the addition of the *Pace-Session* interaction term, the interaction between *Pace* and *Sesson* had a significant effect on PAR scores at the moderate pace level (t-value = 2.76, $p = 0.0059$) and at the slow pace level (t-value = 2.51, $p = 0.0123$). This finding indicates that the difference in PAR scores between a fast and moderate pace was greater when subjects were tested during Session 2 than when tested during Session 1. Under these circumstances, PAR scores increased an additional 0.022 PAR units ($p = 0.0059$)—for a total of 0.055 PAR units or 47 percent—when tested at a moderate pace during Session 2. Likewise, when tested at a slow pace during Session 2, PAR scores increased an additional 0.020 PAR units ($p = 0.0123$), for a total of 0.11 PAR units or 90 percent.

The results reported previously describe the influences of terms across subjects without discussing the by-subject variability. In addition to the random intercept, the final two models incorporated subject-specific slopes: the first for the fixed effect *Session* and the second for the fixed effect *Speed*. Results from the *Session*-based random-slope model estimated a by-subject intercept with standard deviation of 0.0560 PAR units and a standard deviation of 0.0443 PAR units was estimated, corresponding to the variability in slope across subjects. Likewise, the *Speed*-based random-slope model estimated a by-subject intercept with standard deviation of 0.0267 PAR units and a by-subject slope with standard deviation of 0.0270 PAR units and 0.0336 PAR units for fast-to-moderate and fast-to-slow, respectively. Table 10 provides an example of the output produced by the *Session*-based random-slope model, listing intercept and session-specific coefficients as they vary by subject. The inclusion of a random effect term is discussed more thoroughly in the *Discussion* section.

Table 10: Session-specific random-slope model coefficients

	Intercept	Session
S10	0.169	-0.0724
S11	0.0658	-0.00947
S22	0.175	-0.0479
S23	0.128	-0.00546
S24	0.152	-0.0330
S27	0.085	0.000624
S50	0.106	0.0124
S56	0.138	-0.0483
S60	0.188	-0.0180
S63	-0.0351	0.100
S68	0.111	-0.0504
S74	0.0434	0.0507
S83	0.144	0.0184
S86	0.108	0.0219
S89	0.113	0.00219
*Coefficients fixed across subjects: Moderate Pace = 0.0386; Slow Pace = 0.0803; Moderate Pace - Session = 0.0181; Slow Pace - Session = 0.0257.		

Overall, it has been shown that average PAR score across subjects did not significantly change across testing session. However, the inclusion of the by-subject random slope term indicated that the PAR scores of some subjects may have varied more from the first to the second testing session than other subjects. Following a 95 percent confidence interval, the

subjects' intercepts in the *Session*-based random-slope model were expected to vary between 0.0029 to 0.22 PAR units (±1.96sd from the population average PAR) and slopes were expected to range from -0.092 to 0.082 PAR units/session. These rough estimates are confirmed by generated output presented in Table 10, showing how the coefficient (or slope) varied by subject. About half of the subjects reduced their PAR scores across session, while the remaining half generated increased scores. Subject S63 had the greatest increase across sessions (rose 0.100 PAR units across sessions). This result confirms what was seen across the boxplots presented in Figure 21. It should be noted that Figure 21 reveals that subject S63 produced both the lowest median score and smallest variation between scores, leaving one to question whether this was truly indicative of the subjects performs or, in fact, an erroneous measurement, and whether Session 2 results were a truer representation of the subject's performance.

Treatment Effects

The significance of the baclofen treatment was considered after the unblinding of subject labels. A new fixed effect, *Label*, was incorporated into the previously discussed mixed effect model and was used to distinguish MS subjects from control; however, testing revealed that an MS diagnosis did not have a significant effect on PAR scores (*Label*: $F(1,13) = 0.0147$, $p = 0.905$). Table 11 provides a by-subject breakdown of scores at the baseline scenario (i.e. movements performed at a fast pace, using the left arm) and little or no correlation between scores and the subject's condition is evident. Subjects were ranked in descending order based on their Session 1 PAR scores.

Table 12 provides a more detailed breakdown of clinical and kinematic performance measures across sessions. Average PAR scores were computed for each

Table 11: By-subject Performance Metric Comparison

Subject	Label	Session 1 PAR	Session 2 PAR Change	Session 1 MAS	Session 2 MAS Change
S60	MS	0.188	-0.0180	1	-1
S22	C	0.175	-0.0479	1	-0.5
S10	MS	0.169	-0.0724	0.5	-0.5
S24	C	0.152	-0.0330	0	0
S83	MS	0.144	0.0184	2.5	-1.5
S56	MS	0.138	-0.0483	0	0.5
S23	C	0.128	-0.00546	0	0
S89	MS	0.113	0.00219	1.5	-1
S68	MS	0.111	-0.0504	0.875	0.125
S86	MS	0.108	0.0219	1.5	-1
S50	C	0.106	0.0124	0	0
S27	C	0.085	0.000624	0	0
S11	C	0.0658	-0.00947	0	0
S74	MS	0.0434	0.0507	-	-

Table 12: MS Subject Performance Measures Pre-, Post- Treatment

	MS			Control		
Measure	**Session 1**	**Session 2**	**p-value**	**Session 1**	**Session 2**	**p-value**
PAR						
Slow	0.21 ± 0.058	0.23 ± 0.040	0.476	0.21 ± 0.038	0.21 ± 0.035	0.616
Mod	0.18 ± 0.045	0.17 ± 0.050	0.803	0.15 ± 0.044	0.17 ± 0.038	0.309
Fast	0.12 ± 0.050	0.12 ± 0.041	0.897	0.13 ± 0.045	0.10 ± 0.026	0.257
MAS						
	1.0 ± 0.96	0.72 ± 0.71	0.0499	0.17 ± 0.38	0.083 ± 0.28	--
TS*						
V1	0.59 ± 0.71	0.44 ± 0.72	0.363	0 ± 0	0 ± 0	--
V2	1.0 ± 0.98	0.53 ± 0.76	0.0250	0.083 ± 0.28	0.083 ± 0.28	--
V3	1.3 ± 1.1	1.0 ± 0.74	0.207	0.17 ± 0.38	0.083 ± 0.28	--

NOTE – Measures reported as mean ± std

*V1 – slow movement; V2 – under effects of gravity; V3 – fast movement

subject, pace and session and compared using a paired t-test to reconfirm PAR scores did not significantly differ between sessions at each of the three paces. It was found that for all cases—slow, moderate, and fast—the mean difference between PAR scores during Session 1 to Session 2 was not significant (*Slow*: t = 0.753, p = 0.476 *Moderate*: t = 0.259, p = 0.803; *Fast*: t = 0.134, p = 0.897). Clinical performance measures were compared using the Wilcoxon Rank Sum Test, for reasons previously discussed. Improvement in TS scores assessed under gravity were significant, as well as arguably significant MAS scores (TS V2: V = 162, p = 0.0250; MAS: V = 577, p = 0.0499).

Discussion

Tools for Intra- and Inter-subject Comparison

As demonstrated in Figure 20 and Figure 22, dynamical phase portraits and PAR results provided a repetition-by-repetition visual record of each subject's performance, an advantage that is intangible when assessment is purely subjective. Lattice plots, in particular, provided the added benefit of comparing the simultaneous effects of multiple factors on PAR scores. These tools were simplistic, yet invaluable, and, in conjunction with regression models, were necessary for drawing comparisons within and across subjects.

Mixed effect regression models allow researchers to consider inter-subject variability while drawing conclusions about the general population (Bates et al. 2014, Bates D 2015). The incorporation of random effect term acknowledges the existence of baseline differences across the subject pool, and therefore, the intercepts for these terms are expected to vary (referred to in literature as *random intercept*), whereas the session (1

or 2), side (right or left) and pace (slow, moderate or face) tested remained constant for all subjects.

The random effect term within the final models incorporated both a random intercept and random slope (tested both *Session*-based and *Speed*-based random-slope models). In doing so, it was expected that each subject varied uniquely from the baseline average and responded differently across testing sessions and movement pace. Both random-slope models allowed for correlation between the random intercept and random slope of each subject, so for instance, it was anticipated that if a subject had a higher initial PAR score, then multiple testing sessions or changes in pace—from fast to moderate to slow—would have a greater effect on the subject's PAR scores (Bates et al. 2014, Bates D 2015). This may have been an unwarranted assumption, and uncorrelated random effects may be more appropriate.

For this particular study, the side used during testing was not a significant factor on PAR scores ($p = 0.326$), although studies have shown MS subjects may present with upper limb hemiparesis, requiring treatment (Mark et al. 2008). It is important to note that hemiparesis is highly prevalent in other neurological disorders, including cerebral palsy and stroke; it is hypothesized that *Side* would be a significant factor in studies involving these populations and useful for tracking patient progression through therapy (Stoykov and Corcos 2009, Rostami et al. 2012).

Treatment Effects

The kinematic performance measure, PAR, did not improve significantly between the baseline test session and the one-month follow up test session, although a significant

improvement was observed in some clinician measures. This finding may be reasoned several ways.

For one, the clinician performance measures are subjective, and therefore, their reliability between raters, or even that of a single rater testing at two distinct sessions, is less certain. It is possible that the anticipated improvement in smoothness, knowing that an anti-spastic medication had been administered, may have influenced how the rater perceived the subject's motion.

Alternatively, the PAR metric, in its current form, may not be assigning appropriate weight to irregular features of a phase portrait, such as inner loops. Thus, a reworking of the formula may help emphasize nuances in movement and differentiate levels in impairment.

Lastly, it is important to note that MS is known to have a greater effect on lower limb function than on upper limbs (Feinstein, Freeman, and Lo 2015). Therefore, it is not alarming that this study did not find the treatment efficacy to be greater when the upper limb was only considered. If the methods and analysis were repeated using data generated from lower extremities rather than upper, a greater discrepancy between MS and control baseline PAR scores is expected. It is also anticipated that the PAR metric will have a greater difference before and after treatment and correlate with the treatment plan.

Pace-dependencies

The mixed-effect linear regression model showed that PAR scores were most dependent on movement pace; pace-dependencies became even more prominent during

Session 2. In most cases, the differences are substantial and can be seen through visual inspection of a subject's phase portraits (Figure 20) and lattice plots (Figure 22).

Wel, et. al. studied the effects of movement speed—particularly movements generated at slow speed and hypothesized that people had a general preference to adjust the frequency of their movements until the frequency coincided with a natural resonance frequency. The group found that the number of velocity peaks within a kinematic profile and dwell time were directly proportional to the movement period, while peak velocity was, unsurprisingly, indirectly proportional to the length of the movement period. Therefore, it was concluded that when subjects moved slower than naturally preferred, the speed of their trajectory is not only slowed, but the onset of the trajectory was also delayed and required more submovements to complete (van der Wel, Sternad, and Rosenbaum 2010).

Consideration toward the peak velocity or delay in movement was not given in the present study, since the protocol required visual tracking to promote intra- and inter-subject consistency. However, the presence of multiple, unexpected peaks in the kinematic profiles (i.e. velocity-time graph) indicated that participants (both MS and control) experienced the same movement phenomena—the tendency to divide a trajectory into multiple submovements when movements were generated slower than the preferred frequency.

The lattice plot (Figure 22) showed that some subjects had a more distinct increase in PAR scores as the movement pace slowed than others. Some trials—for example S86/Session1/Right Arm—were void of this steady increase in scores, but the slope between fast to slow scores became more defined in Session 2. This result

provokes the question of whether a distinct slope may actually be an indication of improved motor performance.

Limitations of Study

Mixed effect modeling has become a more common practice across various fields of study due to its flexibility to consider simultaneous effects of factors, deal with repeated measures or missing data, and adjust for heteroscedasticity (Baayen 2008). Additionally, continual software development, including that which is open-source, has encouraged its use. However, as often the case with development, advanced features are often gained at the loss of others. The models development in the present study initially utilized R's *lme4* package functionality, specifically the *lmer* function and supporting test functions. However, with the existing heteroscedasticity among data points, the capabilities of the *lme4* package were traded for the less recent mixed modeling package, *nlme*, in order to incorporate weighted variance terms within the model. Testing fixed and random effect combinations was limited while using the *nmle* package due to the failed convergence of many models. Visual inspections of residual scatter plots showed improvement in homoscedasticity; however, it is important to note that minimal fanning of points remains, and so a slight bias is expected. It is also important to note that this modeling scheme was designed to study how factors affected performance and was not intended to predict PAR scores based on the existing factors.

Conclusions

Demonstrated by the present study, PAR is a viable metric to quantify human movement and is a useful tool for tracking progression of impaired function over

treatment sessions, as well as capturing and assessing the idiosyncrasies of movement. PAR did not improve significantly between the baseline test session and the one-month follow up test session, as the case for most clinician-based scores (MAS and TS). Future studies, especially those involving MS patients, should assess other single-joint movements, such as those involving the lower extremities. A reformulation of the PAR metric may place greater weight on phase portrait anomalies, such as inner loops, which may improve the differentiation of movement types.

CHAPTER 5: GENERAL CONCLUSIONS

Limitations

Several groups have drawn attention to a significant issue surrounding spasticity; spasticity is vaguely defined and often misinterpreted, resulting in test protocols and measurement tools that have been deemed inadequate (Malhotra et al. 2009, Pandyan et al. 2005, Burridge et al. 2005). As a result of this unsettled discussion of an appropriate definition for spasticity, aspects of the protocol used herein come into question.

Burridge, et al. highlighted protocol strategies and discussed how strategic discrepancies—such as compromising advancements in research for cost-effective, practical assessments and vice versa—arise depending on whether the studies are research or clinically driven (Burridge et al. 2005). The strategy behind the protocol used within this thesis, for testing voluntary motion, was guided by the definition proposed by the SPASM Coalition; therefore, the protocol was not limited by Lance's definition but rather is guided by a definition that is arguably vague.

Groups have advocated that UMN syndrome is best examined by multifaceted test protocols (Burridge et al. 2005, van der Krogt et al. 2012). The present thesis may have been limited by the exclusively active protocol. The voluntary motion test protocol excluded subjects with severe paresis and spasticity, as well as individuals with cognitive impairment. For these individuals, spasticity assessment must be based solely on involuntary motion protocols.

Justification of Thesis

Despite concerns that may arise, it must be emphasized that phase profiles—an underutilized graphing tool used to display the kinematic data—provides an opportunity to gain insight in spasticity that is otherwise hidden by conventional temporal plots. The present thesis investigated the dynamic behavior of single-joint elbow extension and flexion, while analyzing and comparing metrics that may be used to quantify the complexity of these movements.

This thesis focused on spasticity, with the goal of advancing clinical diagnostic treatment protocols. Thus, spasticity was approached from a direction that, in this day, is common and appealing from a clinical perspective; the testing device and software is economically feasible to reproduce and clinically realistic (i.e. simple enough for a clinician to use and appropriate to house in a clinic setting), although it may actually measure a blend of UMN syndrome positive features at the expense of advancing research in spasticity, specifically.

The outcome of this thesis is expected to benefit and appeal to clinical settings but, nonetheless, will set a foundation for future studies; suggestions are provided, regarding how to adapt the device and protocol, to advance research of spasticity and other symptoms of UMN syndrome. Justification of the present thesis was three-fold:

1. Graphing kinematic data in the phase domain provided a valuable and progressive tool for viewing and quantifying the performance of both hemiparetic patients and those suffering from spasticity.
2. Testing under an active-motion protocol offered insight into impaired motion that may not have surfaced during conventional passive protocols.

3. The device and software used in this thesis are both cost-effective and easily reproducible for a clinical setting. Adapting the device to be even more economically feasible, portable, etc., allowing patients to complete at-home treatment and assessment, is a realistic task and is recommended as future work.

Recommendations for Future Work

Incorporating active and passive-motion protocols may be beneficial and provide more information regarding biomechanical aspects of disorders (Pandyan et al. 2005, Burridge et al. 2005, van der Krogt et al. 2012). In the SPMS study presented in Chapter 4, passive test scores were assessed by clinicians using MAS and TS, but it is recommended that future work focuses on developing a passive-MAST test, in which a servomotor drives the subject's arm and a force transducer measures the resistance to movement. The protocol used within this thesis focused on the motion kinematics but disregarded dynamics. Adapting the MAST to incorporate a servomotor and modifying the test protocol will provide insight into the forces and torques driving the motion and show how the dynamics vary from healthy to impaired subjects. In addition, electromyographical (EMG) recordings of agonist/antagonist activation during the extension-flexion tasks will aid in distinguishing neurogenic and biomechanic contributions, while providing insight into such things as co-activation patterns (Wood et al. 2005).

A limitation of the present thesis was that the generated kinematic phase profiles were somewhat ambiguous, and it was not definitive whether irregular phase portraits were a direct result of spasticity, another UMN syndrome positive feature, or a combination of features; opposing this concern, however, is the added benefit that phase

profiles may accentuate characteristics of UMN syndrome positive features and help to distinguish the disorder, or combination of disorders, responsible for a subject's impaired movement; although beyond the scope of this study, it is recommended that future work focuses on differentiating various features of UMN symptoms.

Additional work is suggested in the development of upper-limb musculoskeletal models that will promote a greater understanding of how motor impairments, such as spasticity, affect muscle behavior and joint kinematics. Valero-Cuevas, et al. discuss many aspects of computational models—including the practicality of and strategies associated with various modeling methods, a description of common learning and control schemes, and the benefits of graphical and computational packages—and express that decisions surrounding computations models lie within creating a balance between "physiological reality and modeling simplicity." The group also emphasizes the need for investigating musculoskeletal models, which simulate motion generated by an impaired, rather than healthy, motor command (Valero-Cuevas FJ et al. 2009).

Moving forward from this thesis, future development of musculoskeletal models will demonstrate how parameters (i.e. stiffness, length, and muscle excitation) affect motion. Models will help verify the cause of complex features, commonly seen in impaired motion, AV and VP phase portraits, and how tuning parameters, such as stiffness, affects the linearity of an AP portrait and the slope of the linear region.

REFERENCES

Alexander, R. M. 1997. "A minimum energy cost hypothesis for human arm trajectories." *Biol Cybern* 76 (2):97-105.

Alibiglou, L., W. Z. Rymer, R. L. Harvey, and M. M. Mirbagheri. 2008. "The relation between Ashworth scores and neuromechanical measurements of spasticity following stroke." *Journal of Neuroengineering and Rehabilitation* 5.

Alt Murphy, M., C. Willen, and K. S. Sunnerhagen. 2011. "Kinematic variables quantifying upper-extremity performance after stroke during reaching and drinking from a glass." *Neurorehabil Neural Repair* 25 (1):71-80.

Ansari, N. N., S. Naghdi, S. Hasson, M. H. Azarsa, and S. Azarnia. 2008. "The Modified Tardieu Scale for the measurement of elbow flexor spasticity in adult patients with hemiplegia." *Brain Injury* 22 (13-14):1007-1012.

Atler, T., W. Craelius, M. Wininger, M. Wallin, and M. Moradi. 2015. "Quantitative Study on Effects of Baclofen on Muscle Spasticity in Multiple Sclerosis." NEBEC, Rensselaer Polytechnic Institute.

Baayen, R.H, Davidson, D.J., Bates, D.M. 2008. "Mixed-effects modeling with crossed random effects for subjects and items." 59 (4):390–412.

Bandi, Surendra, and Anthony Ward. 2010. Spasticity. In *International Encyclopedia of Rehabilitation*. University at Buffalo, The State University of New York: Center for International Rehabilitation Research Information and Exchange.

Barnes, Michael, and Garth Johnson. 2008. *Upper Motor Neurone Syndrome and Spasticity: Clinical Management and Neurophysiology*. Second ed: Cambridge University Press.

Bartlett, M. S. 1937. "Properties of Sufficiency and Statistical Tests." *Royal Society of London Proceedings Series A* 160:268-282.

Bates D, Maechler M, Bolker BM and Walker S. 2015. "lme4: : Linear mixed-effects models using Eigen and S4." *submitted to Journal of Statistical Software*.

Bates, Douglas, Martin Maechler, Ben Bolker, and Steven Walker. 2014. "lme4: Linear Mixed-Effects Models using Egen and S4." http://cran.r-project.org/web/packages/lme4/citation.html.

Beard, S., A. Hunn, and J. Wight. 2003. "Treatments for spasticity and pain in multiple sclerosis: a systematic review." *Health Technol Assess* 7 (40):iii, ix-x, 1-111.

Bensmail, Djamel, Johanna V. G. Robertson, Christophe Fermanian, and Agnes Roby-Brami. 2010. "Botulinum Toxin to Treat Upper-Limb Spasticity in Hemiparetic Patients: Analysis of Function and Kinematics of Reaching Movements." *Neurorehabilitation and Neural Repair* 24 (3):273-281.

Bernstein, N. 1967. The co-ordination and regulation of movements. Oxford: Pergamon Press.

Berret, B., E. Chiovetto, F. Nori, and T. Pozzo. 2011. "Evidence for Composite Cost Functions in Arm Movement Planning: An Inverse Optimal Control Approach." *Plos Computational Biology* 7 (10).

Beuter, A, and A Garfinkel. 1985. "Phase Plane Analysis of Limb Trajectories in Nonhandicapped and Cerebral Palsied Subjects." *Adapted Physical Activity Quarterly* 2:214-227.

Bohannon, R. W., and M. B. Smith. 1987. "Interrater reliability of a modified Ashworth scale of muscle spasticity." *Phys Ther* 67 (2):206-7.

Burridge, J. H., D. E. Wood, H. J. Hermens, G. E. Voerman, G. R. Johnson, F. van Wijck, T. Platz, M. Gregoric, R. Hitchcock, and A. D. Pandyan. 2005. "Theoretical and methodological considerations in the measurement of spasticity." *Disabil Rehabil* 27 (1-2):69-80.

Canós, Antoni J. 2006. Fast and Robust Self-intersections. File Exchange-MATLAB Central: The MathWorks, Inc.

Chang, J.-J., F.-C. Su, Y.-S. Yang, L.-Y. Guo, and W.-L. Wu. 2008. "Differences in reaching performance between normal adults and patients post stroke-a kinematic analysis." *Journal of Medical and Biological Engineering* 28 (1):53-58.

Clark, J. E., and S. J. Phillips. 1993. "A longitudinal study of intralimb coordination in the first year of independent walking: a dynamical systems analysis." *Child Dev* 64 (4):1143-57.

Cozens, J. A., and B. B. Bhakta. 2003. "Measuring movement irregularity in the upper motor neurone syndrome using normalised average rectified jerk." *J Electromyogr Kinesiol* 13 (1):73-81.

de Sa, J. C. C., L. Airas, E. Bartholome, N. Grigoriadis, H. Mattle, C. Oreja-Guevara, J. O'Riordan, F. Sellebjerg, B. Stankoff, K. Vass, A. Walczak, H. Wiendl, and B. C. Kieseier. 2011. "Symptomatic therapy in multiple sclerosis: a review for a multimodal approach in clinical practice." *Ther Adv Neurol Disord* 4 (3):139-68.

Detrembleur, C., F. Dierick, G. Stoquart, F. Chantraine, and T. Lejeune. 2003. "Energy cost, mechanical work, and efficiency of hemiparetic walking." *Gait Posture* 18 (2):47-55.

DiBerardino, L. A., J. D. Polk, K. S. Rosengren, J. B. Spencer-Smith, and E. T. Hsiao-Wecksler. 2010. "Quantifying complexity and variability in phase portraits of gait." *Clin Biomech (Bristol, Avon)* 25 (6):552-6.

Edelsbrunner, H D., D.G. Kirkpatrick, and R Seidel. 1983. "On the shape of a set of points in the plane." I*EEE Trans. Inform. Theory* ***IT-29:***551-559.

Edelsbrunner, H., and E.P. Mücke. 1994. "Three-Dimensional Alpha Shapes." A*CM Trans. Graph* 13 (1):43-72.

Eucker, S. A., J. B. Lisauskas, J. Singh, and S. J. Kovacs. 2001. "Phase plane analysis of left ventricular hemodynamics." J*ournal of Applied Physiology* 90 (6):2238-2244.

Feinstein, A., J. Freeman, and A. C. Lo. 2015. "Treatment of progressive multiple sclerosis: what works, what does not, and what is needed." L*ancet Neurol* 14 (2):194-207.

Fleuren, J. F. M., G. E. Voerman, C. V. Erren-Wolters, G. J. Snoek, J. S. Rietman, H. J. Hermens, and A. V. Nene. 2010. "Stop using the Ashworth Scale for the assessment of spasticity." J*ournal of Neurology Neurosurgery and Psychiatry* 81 (1):46-52.

Foran, J. R. H., S. Steinman, I. Barash, H. G. Chambers, and R. L. Lieber. 2005. "Structural and mechanical alterations in spastic skeletal muscle." D*evelopmental Medicine and Child Neurology* 47 (10):713-717.

Go, A. S., D. Mozaffarian, V. L. Roger, E. J. Benjamin, and et al. 2014. "Executive summary: heart disease and stroke statistics--2014 update: a report from the American Heart Association." C*irculation* 129 (3):399-410.

Goldvasser, D., C. A. McGibbon, and D. E. Krebs. 2001. "High curvature and jerk analyses of arm ataxia." B*iol Cybern* 84 (2):85-90.

Govindan, Rathinaswamy B., Srinivasan Vairavan, Bhargavi Sriram, James D. Wilson, Hubert Preissl, Hari Eswaran, and Ieee. 2011. "Phase plane based identification of fetal heart rate patterns." 2*011 Annual International Conference of the Ieee Engineering in Medicine and Biology Society (Embc):*1455-1458.

Graham, R.L. 1972. An efficient algorith for determining the convex hull of a finite planar set. In I*nformation Processing Letters:* North-Holland Publishing Company.

Guiard, Y. 1993. "On Fitt and Hooke Laws - Simple Harmonic Movement in Upper-Limb Cyclical Aiming." A*cta Psychologica* 82 (1-3):139-159.

Haas, Bernhard M, and J Lesley Crow. 1995. "Towards a Clinical Measurement of Spasticity?" P*hysiotherapy* 81 (8):474-479.

Hefter, Harald, Wolfgang H. Jost, Andrea Reissig, Benjamin Zakine, Abdel Magid Bakheit, and Joerg Wissel. 2012. "Classification of posture in poststroke upper limb spasticity: a potential decision tool for botulinum toxin A treatment?" I*nternational Journal of Rehabilitation Research* 35 (3).

Hurmuzlu, Y., C. Basdogan, and J. J. Carollo. 1994. "Presenting Joint Kinematics of Human Locomotion using Phase Plane Portraits and Poincare Maps." J*ournal of Biomechanics* 27 (12):1495-1499.

Kistemaker, D. A., J. D. Wong, and P. L. Gribble. 2010. "The central nervous system does not minimize energy cost in arm movements." J *Neurophysiol* 104 (6):2985-94.

Koman, L. A., R. M. M. Williams, P. J. Evans, R. Richardson, M. J. Naughton, L. Passmore, and B. P. Smith. 2008. "Quantification of upper extremity function and range of motion in children with cerebral palsy." D*evelopmental Medicine and Child Neurology* 50 (12):910-917.

Krach, L. E. 2001. "Pharmacotherapy of spasticity: oral medications and intrathecal baclofen." J *Child Neurol* 16 (1):31-6.

Lance, J. W. 1980. "The control of muscle tone, reflexes, and movement: Robert Wartenberg Lecture." N*eurology* 30 (12):1303-13.

Latash, M. L., J. P. Scholz, and G. Schoner. 2002. "Motor control strategies revealed in the structure of motor variability." E*xerc Sport Sci Rev* 30 (1):26-31.

Liang, J., H. Edelsbrunner, P. Fu, P. V. Sudhakar, and S. Subramaniam. 1998. "Analytical shape computation of macromolecules: I. Molecular area and volume through alpha shape." P*roteins* 33 (1):1-17.

Lundgren, Jonas. 2010. Alpha shapes. In A*lpha shape of 2D/3D point set.* File Exchange-MATLAB Central: The MathWorks, Inc.

Lundstrom, E., A. Smits, J. Borg, and A. Terent. 2010. "Four-Fold Increase in Direct Costs of Stroke Survivors With Spasticity Compared With Stroke Survivors Without Spasticity The First Year After the Event." S*troke* 41 (2):319-324.

Malhotra, S., A. D. Pandyan, C. R. Day, P. W. Jones, and H. Hermens. 2009. "Spasticity, an impairment that is poorly defined and poorly measured." In C*lin Rehabil*, 651-8. England.

Mark, V. W., E. Taub, K. Bashir, G. Uswatte, A. Delgado, M. H. Bowman, C. C. Bryson, S. McKay, and G. R. Cutter. 2008. "Constraint-Induced Movement therapy can improve hemiparetic progressive multiple sclerosis. Preliminary findings." M*ult Scler* 14 (7):992-4.

Mehtätalo, Lauri. 2013. L*inear mixed-effects models with examples in R*. University of Eastern Finland.

Pandyan, A. D., M. Gregoric, M. P. Barnes, D. Wood, F. Van Wijck, J. Burridge, H. Hermens, and G. R. Johnson. 2005. "Spasticity: Clinical perceptions, neurological realities and meaningful measurement." D*isability and Rehabilitation* 27 (1-2):2-6.

Pandyan, A. D., G. R. Johnson, C. I. Price, R. H. Curless, M. P. Barnes, and H. Rodgers. 1999. "A review of the properties and limitations of the Ashworth and modified Ashworth Scales as measures of spasticity." C*lin Rehabil* 13 (5):373-83.

Physicians, Royal College of. 2009. Spasticity in adults: management using botulinum toxin. National guidelines. edited by Chartered Society of Physiotherapy British Society of Rehabilitation Medicine, Association of Chartered Physiotherapists Interested in Neurology. London: Royal College of Physicians.

Pinheiro, J, and D Bates. 2000. M*ixed-Effects Models in S and S-PLUS (Statistics and Computing)*. 1st ed: Springer.

Pinheiro J, Bates D, DebRoy S, Sarkar D and R Core Team. 2015. nlme: : Linear and Nonlinear Mixed Effects Models. R package version 3.1-120.

Polk, J. D., J. Spencer-Smith, L. DiBerardino, D. Ellis, M. Downen, and K. S. Rosengren. 2008. "Quantifying variability in phase portraits: Application to gait ontogeny." I*nfant Behavior & Development* 31 (2):302-306.

Pousson, M., R. Lepers, and J. Van Hoecke. 2001. "Changes in isokinetic torque and muscular activity of elbow flexors muscles with age." E*xp Gerontol* 36 (10):1687-98.

Przyborowski, J, and H Wilenski. 1940. "Homogeneity of Results in Testing Samples from Poisson Series: with an Application to Testing Clover Seed for Dodder." B*iometrika* 31 (3-4):313-323.

Rekand, T. 2010. "Clinical assessment and management of spasticity: a review." A*cta Neurologica Scandinavica* 122:62-66.

Riley, P. O., B. J. Benda, K. M. Gillbody, and D. E. Krebs. 1995. "Phase Plane Analysis of Stability in Quiet Standing." J*ournal of Rehabilitation Research and Development* 32 (3):227-235.

Rizzo, M. A., O. C. Hadjimichael, J. Preiningerova, and T. L. Vollmer. 2004. "Prevalence and treatment of spasticity reported by multiple sclerosis patients." M*ult Scler* 10 (5):589-95.

Rohrer, B., S. Fasoli, H. I. Krebs, R. Hughes, B. Volpe, W. R. Frontera, J. Stein, and N. Hogan. 2002. "Movement smoothness changes during stroke recovery." J *Neurosci* 22 (18):8297-304.

Rohrer, B., S. Fasoli, H.I. Krebs, N. Hogan, B. Volpe, W.R. Frontera, and J. Stein. 2004. "Submovements grow larger, fewer, and more blended during stroke recovery." I*n: Motor Control.* 8 (4):472-483.

Rostami, H. R., A. A. Arastoo, S. J. Nejad, M. K. Mahany, R. A. Malamiri, and S. Goharpey. 2012. "Effects of modified constraint-induced movement therapy in virtual environment on upper-limb function in children with spastic hemiparetic cerebral palsy: a randomised controlled trial." In N*euroRehabilitation,* 357-65. Netherlands.

Sarkar, Deepayan. 2008. L*attice: Multivariate Data Visualization with R.* New York: Springer.

Sawa, G. M., and D. W. Paty. 1979. "The use of baclofen in treatment of spasticity in multiple sclerosis." C*an J Neurol Sci* 6 (3):351-4.

Scheinberg, A., K. Hall, L. T. Lam, and S. O'Flaherty. 2006. "Oral baclofen in children with cerebral palsy: a double-blind cross-over pilot study." J *Paediatr Child Health* 42 (11):715-20.

Serra, A., K. Liao, M. Matta, and R. J. Leigh. 2008. "Diagnosing disconjugate eye movements - Phase-plane analysis of horizontal saccades." N*eurology* 71 (15):1167-1175.

Singh, Anupa, Aimee Stewart, Denise Franzsen, and Marilyn MacKay-Lyons. 2011. "Energy expenditure of dressing in patients with stroke." I*nternational Journal of Therapy & Rehabilitation.*

Smith, C. R., N. G. LaRocca, B. S. Giesser, and L. C. Scheinberg. 1991. "High-dose oral baclofen: experience in patients with multiple sclerosis." N*eurology* 41 (11):1829-31.

Solari, A., G. Filippini, P. Gasco, L. Colla, A. Salmaggi, L. La Mantia, M. Farinotti, M. Eoli, and L. Mendozzi. 1999. "Physical rehabilitation has a positive effect on disability in multiple sclerosis patients." N*eurology* 52 (1):57-62.

Song, R., K. Y. Tong, and X. L. Hu. 2008. "Evaluation of velocity-dependent performance of the spastic elbow during voluntary movements." A*rch Phys Med Rehabil* 89 (6):1140-5.

Stoykov, M. E., and D. M. Corcos. 2009. "A review of bilateral training for upper extremity hemiparesis." O*ccup Ther Int* 16 (3-4):190-203.

Strogatz, Steven H. 1994. N*onlinear Dynamics And Chaos: With Applications To Physics, Biology, Chemistry, And Engineering (Studies in Nonlinearity).* Cambridge: Perseus Books Publishing.

Team, R Core. 2013. R: A language and environment for statistical computing. Vienna, Austria: R Foundation for Statistical Computing.

Urban, P. P., T. Wolf, M. Uebele, J. J. Marx, T. Vogt, P. Stoeter, T. Bauermann, C. Weibrich, G. D. Vucurevic, A. Schneider, and J. Wissel. 2010. "Occurence and clinical predictors of spasticity after ischemic stroke." S*troke* 41 (9):2016-20.

Valero-Cuevas FJ, Hoffmann H, Kurse MU, Kutch JJ, and Theodorou EA. 2009. "Computational models for neuromuscular function. ." I*EEE Reviews in Biomedical Engineering* 2: 110-35.

van der Krogt, H. J. M., C. G. M. Meskers, J. H. de Groot, A. Klomp, and J. H. Arendzen. 2012. "The gap between clinical gaze and systematic assessment of movement disorders after stroke." J*ournal of Neuroengineering and Rehabilitation* 9.

van der Wel, R. P., D. Sternad, and D. A. Rosenbaum. 2010. "Moving the arm at different rates: slow movements are avoided." J *Mot Behav* 42 (1):29-36.

Watkins, C. L., M. J. Leathley, J. M. Gregson, A. P. Moore, T. L. Smith, and A. K. Sharma. 2002. "Prevalence of spasticity post stroke." C*linical Rehabilitation* 16 (5):515-522.

Wilcoxon, Frank. 1945. "Individual Comparisons by Ranking Methods." B*iometrics Bulletin* 1 (6):80-83.

Wininger, M., N. H. Kim, and W. Craelius. 2009. "Spatial resolution of spontaneous accelerations in reaching tasks." J *Biomech* 42 (1):29-34.

Wininger, M., N. H. Kim, and W. Craelius. 2012. "Reformulation in the phase plane enhances smoothness rater accuracy in stroke." J *Mot Behav 4*4 (3):149-59.

Winstein, C. J., J. P. Miller, S. Blanton, E. Taub, G. Uswatte, D. Morris, D. Nichols, and S. Wolf. 2003. "Methods for a multisite randomized trial to investigate the effect of constraint-induced movement therapy in improving upper extremity function among adults recovering from a cerebrovascular stroke." Ne*urorehabil Neural Repair 1*7 (3):137-52.

Wood, D. E., J. H. Burridge, F. M. Van Wijck, C. McFadden, R. A. Hitchcock, A. D. Pandyan, A. Haugh, J. J. Salazar-Torres, and I. D. Swain. 2005. "Biomechanical approaches applied to the lower and upper limb for the measurement of spasticity: A systematic review of the literature." Di*sability and Rehabilitation 2*7 (1-2):19-32.

Zuur, A., Ieno, E.N., Walker, N., Saveliev, A.A., Smith, G.M. 2009. Mi*xed Effects Models and Extensions in Ecology with R:* Springer Science & Business Media.